In a circuit necessary for cognition and emotional affect, Alzheimer's-like pathology associates with neuroinflammation, cognitive and motivational deficits in the young adult TgF344-AD rat

Caesar M. Hernandez [a,b,*], Macy A. McCuiston [a], Kristian Davis [a], Yolanda Halls [a], Juan Pablo Carcamo Dal Zotto [a], Nateka L. Jackson [b,c], Lynn E. Dobrunz [d], Peter H. King [e,f], Lori L. McMahon [b,c,**]

[a] Department of Medicine, Division of Gerontology, Geriatrics, and Palliative Care, The University of Alabama at Birmingham, Birmingham, AL, USA
[b] Department of Cell, Developmental, and Integrative Biology, The University of Alabama at Birmingham, USA
[c] Department of Neuroscience, Medical University of South Carolina, USA
[d] Department of Neurobiology, The University of Alabama at Birmingham, USA
[e] Department of Neurology, The University of Alabama at Birmingham, USA
[f] Birmingham Veterans Affairs Medical Center, Birmingham, AL, USA

ARTICLE INFO

ABSTRACT

In addition to extracellular amyloid plaques, intracellular neurofibrillary tau tangles, and inflammation, cognitive and emotional affect perturbations are characteristic of Alzheimer's disease (AD). The cognitive and emotional domains impaired by AD include several forms of decision making (such as intertemporal choice), blunted motivation (increased apathy), and impaired executive function (such as working memory and cognitive flexibility). However, the interaction between these domains of the mind and their supporting neurobiological substrates at prodromal stages of AD, or whether these interactions can be predictive of AD severity (individual variability), remain unclear. In this study, we employed a battery of cognitive and emotional tests in the young adult (5–7 mo) transgenic Fisher-344 AD (TgF344-AD; TgAD) rat model of AD. We also assessed whether markers of inflammation or AD-like pathology in the prelimbic cortex (PrL) of the medial prefrontal cortex (mPFC), basolateral amygdala (BLA), or nucleus accumbens (NAc), all structures that directly support the aforementioned behaviors, were predictive of behavioral deficits. We found TgAD rats displayed maladaptive decision making, greater apathy, and impaired working memory that was indeed predicted by AD-like pathology in the relevant brain structures, even at an early age. Moreover, we report that the BLA is an early epicenter of inflammation, and notably, AD-like pathology in the PrL, BLA, and NAc was predictive of BLA inflammation. These results suggest that operant-based battery testing may be sensitive enough to determine pathology trajectories, including neuroinflammation, from early stages of AD.

1. Introduction

Alzheimer's disease (AD) is a neurodegenerative disease characterized by neuronal death, amyloid pathology presenting as extracellular plaques, and hyperphosphorylated tau at various sites, which manifests as intracellular neurofibrillary tangles. Currently, there are over 6 million individuals in the United States (Alzheimer's Association, 2021) and over 55 million individuals worldwide (Gustavsson et al., 2023) diagnosed with AD or related dementia. It is estimated that the economic impact of AD will be 2.8 trillion dollars (U.S.) by 2030 (Wimo et al.,

2015). In addition to the characteristic pathology, several studies have described peripheral inflammation as co-occurring with AD (Lai et al., 2017), particularly after disease onset. While markers of inflammation in the brain have been identified at later ages in AD patients (Lue et al., 2001) and rodent models of AD (Patel et al., 2005; Wu et al., 2020) in addition to early disease stages (Belfiore et al., 2019; Ceyzériat et al., 2024; Liu et al., 2021; Pascoal et al., 2021; Wright et al., 2013), the degree to which individual variability in intracerebral inflammation influences individual variability in cognition at early stages remains unclear.

Accompanying neuropathological insults, AD is also characterized by impaired episodic memory, executive functioning, and emotional affective disorders. Indeed, it has been recognized that some of the earliest behavioral changes involve emotional affect and include increased irritability (Cerejeira et al., 2012; Koenig et al., 2016), suspiciousness (Mendez et al., 1992), fear (Hamann et al., 2002; Hoefer et al., 2008; Weiss et al., 2008), and apathy, or decreased motivation (Robert et al., 2009). It is well established that in addition to intact executive function, decision making requires emotional processing such as incentive motivation (Maddox and Markman, 2010). AD patients exhibit motivational disturbances, impacting several domains of decision making, such as intertemporal choices (or impulsive choice). Intertemporal choice is a decision-making process involving options between smaller, immediate rewards, or larger, delayed rewards. Relative to healthy controls, patients with AD exhibit altered decision making such that they make more impulsive choices favoring immediate rewards (El Haj et al., 2020, 2022; Geng et al., 2020; Manuel et al., 2020; Thoma et al., 2017). In contrast, others have shown no difference in choice performance between patients with AD and healthy controls (Beagle et al., 2020; Bertoux et al., 2015; Coelho et al., 2017).

In healthy individuals, the relationship between executive functions such as working memory (the temporary maintenance of internal representations derived from external stimuli no longer present in the environment) and cognitive flexibility (the ability to adapt to changes in the environment) has also been characterized (Bobova et al., 2009; Hernandez et al., 2017; Shamosh et al., 2008; Shimp et al., 2015). In patients with AD and related dementias, working memory deficits can differentiate AD patients from patients with other neurodegenerative disorders and non-AD dementia (Albert, 1996). Moreover, working memory can be one early cognitive marker of AD (Baddeley et al., 2017; Morris, 1994; Stopford et al., 2012). Additionally, cognitive flexibility is also impaired such that individuals with AD make significantly more errors in a trail making test (Lafleche and Albert, 1995). However, within the context of AD, the relationship between higher order cognitive processes and emotional affect has not been explicitly determined.

A battery of cognitive and emotional testing has been created for diagnosing mild cognitive impairment (MCI) and AD (Weintraub et al., 2018). Similar testing can be performed in rodent models of AD with the use of operant conditioning that includes decision making, emotional affect or motivation, and executive function tasks. Specifically, we can leverage these tasks to assess function within and between several brain structures at the behavioral and neurobiological levels. Intertemporal choice, motivation, and executive function require an extensive network of cortical and subcortical structures including, but not limited to, the rodent prelimbic (PrL) region of the medial prefrontal cortex (mPFC), basolateral amygdala (BLA), and nucleus accumbens (NAc) (Bailey et al., 2016; Churchwell et al., 2009; Floresco and Magyar, 2006; Floresco et al., 2008b; C. M. Hernandez et al., 2018; Hernandez et al., 2022b; Sloan et al., 2006; Yang et al., 2014).

In the transgenic Fisher344 AD (TgF344-AD; TgAD) rat model of AD (Cohen et al., 2013), we have previously shown aberrant synaptic and neuronal activity within the BLA occurs in post-adolescent young adults and predicts fear extinction impairments (Hernandez et al., 2022a). In this study we expanded the battery of testing in young adults (5–7 months) to assess behavioral performance dependent upon the BLA (intertemporal choice and progressive ratio tasks of decision making and

motivation, respectively). In addition, we included functional testing of the PrL (set-shifting task of cognitive flexibility and delayed match-to-sample task of working memory) and the NAc (intertemporal choice and progressive ratio). We then determined if inflammation and AD-like pathology were present at this early age within these regions. Finally, we determined if any deficits in behavioral performance could be explained, at least in part, by underlying neurobiological deficits such as inflammation and AD-like pathology. In this study, we report that relative to age-matched controls, young adult TgAD rats show maladaptive decision making, greater apathy, and impaired working memory. Furthermore, greater AD-like pathology is predictive of the individual variability in behavioral deficits and neuroinflammation at these early ages.

2. Materials and methods

2.1. Subjects

A total of 33 (see Table 1) wild type (WT) and TgAD rats were used for behavioral and neurobiological experiments. As previously described (Goodman et al., 2021; Smith and McMahon, 2018; Smith et al., 2022), TgAD rats containing the human Swedish mutation amyloid precursor protein (APP^{swe}) and the presenilin-1 exon 9 deletion mutant (PS1$^{\Delta E9}$) were bred with WT F344 females (Envigo: previously Harlan Laboratories) at the University of Alabama at Birmingham. All breeding and experimental procedures were approved by the University of Alabama Institutional Animal Care and Use Committee and follow guidelines set by the National Institutes of Health. The original breeding pair was obtained from University of Southern California, Los Angeles, CA (Cohen et al., 2013). Rats were maintained under standard animal care facility conditions with food (catalog #Harlan 2916, Teklad Diets) and water *ad libitum* and a 12 h reverse light/dark cycle (lights off at 7am) at 22°C and 50% humidity. Rats were housed in standard rat cages (height, 7 inches; floor area, 144 square inches) in same-sex groups of four or less at weights of ~300 g or two per cage when ≥400 g. Rats were aged from birth to experimental age groups categorized as young adults (YA: 5.67–7.59 mo, average of 6.39 mo). Prior to operant conditioning, all rats were single housed and food-restricted to 85% of their free-feeding body weight.

2.2. Operant conditioning

2.2.1. Apparatus

All behavioral experiments were implemented as described in our previous work (Bañuelos et al., 2014; Hernandez et al., 2017; Simon et al., 2010). As previously described, testing was conducted in 4 identical standard rat behavioral test chambers (Coulbourn Instruments) with metal front and back walls, transparent Plexiglas side walls, and a floor composed of steel rods (0.4 cm in diameter) spaced 1.1 cm apart. Each test chamber was housed in a sound-attenuating cubicle and was equipped with a recessed food pellet delivery trough located 2 cm above the floor in the center of the front wall. The trough was fitted with a photobeam to detect head entries and a 1.12 W lamp for illumination. Food rewards consisted of 45-mg grain-based food pellets (PJAI; Test Diet, Richmond, IN, USA). Two retractable levers were positioned to the left and right of the food trough (11 cm above the floor), and a 1.12 W

Table 1
Table of initial and final group numbers.

Genotype	WT		TgAD	
Sex	M	F	M	F
Behavior (initial ns)	9	8	9	7
Behavior (final ns)	6	8	8	6
Protein (initial ns)	6	8	8	6
Protein (Final ns)	6	8	8	6

cue lamp was located 3.8 cm above each lever. An additional 1.12 W house light was mounted near the top of the rear wall of the sound-attenuating cubicle. A computer interfaced with the behavioral test chambers and equipped with Graphic State 4 software (Coulbourn Instruments) was used to control experiments and collect data.

2.2.2. Behavioral shaping

Before the start of testing, rats were food-restricted to 85% of their free-feeding weights over the course of 7 d and maintained at this weight for the duration of testing. Rats progressed through three stages of shaping designed to train them to reliably press each of the two response levers prior to starting task-specific procedures. On the day before Shaping Stage 1, each rat was given five 45 mg food pellets in its home cage to reduce neophobia to the food reward used in the task. Shaping Stage 1 consisted of a 64 min session of magazine training, involving 38 deliveries of a single food pellet with an intertrial interval of 100 ± 40 s. Shaping Stage 2 consisted of lever press training, in which a single lever (left or right, counterbalanced across WT and TgAD rats) was extended and a press resulted in delivery of a single food pellet. After reaching a criterion of 50 lever presses in 30 min, rats were then trained on the opposite lever using the same procedures. During Shaping Stage 3, a nosepoke into the food trough resulted in extension of the left or right lever (counterbalanced across trials in this Stage of testing), and a lever press resulted in a single food pellet delivery. Rats were trained in Shaping Stage 3 until achieving 80 lever presses in a 30 min session.

2.2.3. Procedures for the intertemporal choice task

This task was based on (Cardinal et al., 2001; Evenden and Ryan, 1996), and was used previously to demonstrate age-related alterations in decision making in Fischer 344 rats (Simon et al., 2010). Prior to commencing the intertemporal choice task, rats were trained in an additional shaping protocol to reinforce each lever with a reward outcome. Rats nose poked into the food trough to initiate the extension of one lever (either left or right, randomized within every two trials), and a lever press resulted in a single food pellet. After two consecutive days of 45 presses on each lever, rats were advanced to the final delay discounting task.

Each 80 min session consisted of 5 blocks of 12 trials each (2 forced choices and 10 free choices). Each 80 s trial began with a 10 s illumination of the food trough and house lights. A nosepoke into the food trough during this time extinguished the food trough light and triggered extension of either a single lever (forced choice trials) or of both levers simultaneously (free choice trials). Trials in which rats failed to nose-poke during the 10 s window were scored as omissions. The forced choice trials were designed to remind rats of the delay contingencies in effect for that block. A press on one lever (either left or right, counter-balanced across age groups) resulted in one food pellet (the small reward) delivered immediately. A press on the other lever resulted in 4 food pellets (the large reward) delivered after a variable delay. The identities of the levers remained consistent throughout testing. Failure to press either lever within 10 s of their extension resulted in the levers being retracted and lights extinguished, and the trial was scored as an omission. Once either lever was pressed, both levers were retracted for the remainder of the trial. The duration of the delay preceding large reward delivery increased between each block of trials (0, 10, 20, 40, 60 s), but remained constant within each block.

2.2.4. Procedures for the progressive ratio task

This task evaluated rats' motivation to press a lever to obtain food reward, and was based on a design used previously by our lab and others (Barr and Phillips, 1999; Cetin et al., 2004; Kheramin et al., 2005; Mendez et al., 2009). Instrumental responding for one food reward was assessed using a progressive ratio schedule of reinforcement, on which the number of lever presses required to earn a reward increased with each successive reward earned (1, 3, 6, 10, 15, …). Rats were tested in the progressive ratio task for 3 consecutive sessions (at least one per day). On the fourth session, the food reward size was increased to 4 food rewards per schedule. These sessions varied in length, ending only after 30 min elapsed with no reward delivery.

2.2.5. Procedures for the set shifting task used to assess cognitive flexibility

This task was originally developed by Floresco and colleagues (Floresco et al., 2008a) and was used previously to demonstrate impaired cognitive flexibility in aged Fischer 344 rats (e.g., (Beas et al., 2017, 2013). Rats were first assessed on a protocol designed to determine their individual "side bias" or inherent preference for the left or right lever. This protocol was composed of 45 trials, each of which consisted of two phases. In the first phase of each trial, the house light was illuminated and both levers extended into the test chamber. A response on either lever resulted in retraction of both levers and delivery of a single food pellet. In the second phase of each trial, both levers were extended into the chamber, but only a response on the lever opposite to the choice made in the first phase was rewarded. If the rat made an "incorrect" response (i.e., chose the same lever as in the first phase), the levers were retracted and the house light was extinguished. The second phase of the trial was then repeated until the rat made a correct response, and then a new trial was initiated. An individual rat's "side bias" reflected the lever position on which it made the greatest number of responses across the entire test session.

The day after side bias determination, rats began discrimination training on the initial (visual cue) discrimination learning rule. Each 20 s trial began by illuminating one of the cue lights positioned over the left or right lever for 3 s (the position was randomly selected within each pair of trials). Both levers were then inserted into the chamber for 4 s, during which the cue light remained illuminated (the house light was also illuminated during this phase). If the rat made a correct response (pressed the lever beneath the cue light), both levers were retracted, the cue light was extinguished, and a single food pellet was delivered. If the rat made an incorrect response (pressed the lever opposite from the cue light), the levers were retracted and the house light extinguished, but no food was delivered. As in our previous work (Beas et al., 2013, 2016), rats were trained on the visual cue discrimination for a minimum of 30 trials and until reaching criterion performance of 8 consecutive correct choices. The visual discrimination task included a maximum of 120 trials/session. If a rat failed to reach criterion performance in the course of a single session, the task was repeated on subsequent days. Upon reaching criterion performance, the session was ended. To reinforce the formation of an attentional "set", on the day after reaching criterion performance, rats received one additional session of 120 trials of visual discrimination training.

The day after completing visual cue discrimination training, rats received a "set shift" in which the contingencies for making a correct (reinforced) choice were changed. The presentation of the trials during the set shift was identical to that in the visual cue discrimination phase of the task; however, to receive a food reward, rats were now required to ignore the cue light and instead respond to a particular lever position (either left or right, whichever was not their "biased" side as determined during the side bias assessment) to receive a food reward. Rats were trained on the set shift until achieving criterion performance of 10 consecutive correct trials (Beas et al., 2013, 2017). As in the initial discrimination phase, each session included a maximum of 120 trials.

2.2.6. Procedures for delayed response task used to assess working memory

The design of this task was based on (Sloan et al., 2006), and has been used by our lab previously to demonstrate age-related working memory impairments in F344 rats (e.g., (Bañuelos et al., 2014; Beas et al., 2013; McQuail et al., 2016). Each 40 min session began with illumination of the house light, which remained illuminated throughout the entire session except during timeout periods (see below). Rats received a single test session each day. Each trial in the task began with extension of a single "sample" lever into the chamber (Fig. 1A). The sample lever (left or right) was randomly selected within each pair of
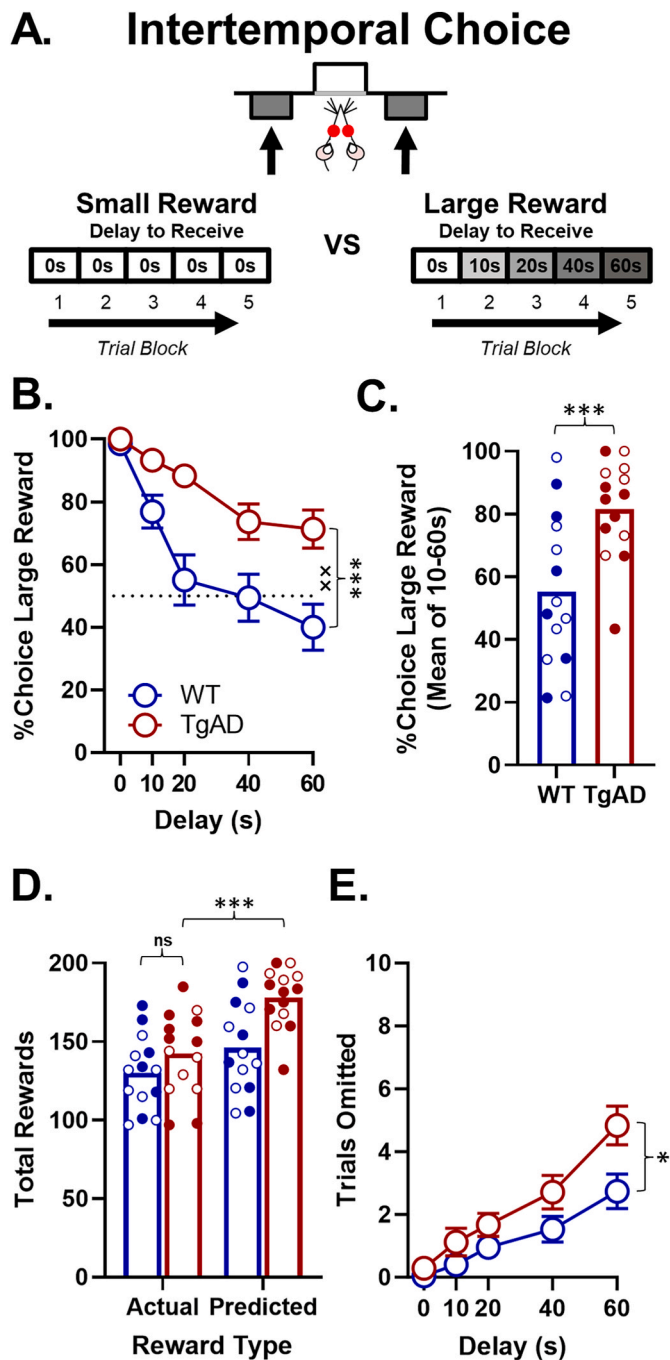
Fig. 1. Intertemporal choice. A. Task schematic of the intertemporal choice task. **B.** Choice of the large, delayed reward was greater in young adult TgAD rats relative to WT controls, particularly at longer delays. **C.** The individual variability of WT and TgAD rats when performance was averaged between 10 and 60 s. TgAD rats had a greater preference for large, delayed rewards. **D.** Despite having a greater preference for the large, delayed reward, TgAD rats did not maximize the number of rewards earned if all trials were completed (actual number of rewards earned vs predicted number of rewards earned). **E.** Total rewards earned was not greater in the TgAD rats due to a greater number of trial omissions. In all panels, *p < 0.05, ***p < 0.001, ××p < 0.01 for the interaction, and ns = not significant; blue represents WT rats, and red represents TgAD rats. Animal numbers in this experiment were n = 14 WT (n = 8 females, n = 6 males) and n = 14 TgAD (n = 6 females, n = 8 males). Females are represented by open circles and males are represented by closed circles. (For interpretation of the references to color in this figure legend, the reader is referred to the Web version of this article.)

trials to ensure equal representation of both levers across the test session. A press on the sample lever caused it to retract and initiated the delay interval. During the delay interval, rats were required to nosepoke into the food trough to minimize their use of mediating strategies (e.g., positioning themselves in front of the sample lever during the delay). The first nosepoke executed after the delay interval expired initiated the "choice" phase, in which both levers were extended. During the choice phase, a response on the same lever pressed during the sample phase was "correct" and resulted in retraction of both levers and delivery of a food pellet into the food trough. A nosepoke into the food trough to retrieve the food initiated a 5 s intertrial interval, after which the next trial began. A response on the opposite lever from that chosen during the sample phase was "incorrect" and resulted in retraction of both levers and initiation of a 5 s "timeout" period during which the house light was extinguished. Immediately following this timeout, the house light was re-illuminated, signaling the start of the next trial.

During initial sessions in this task, there were no delays between the sample and choice phases, and a correction procedure was used such that the sample lever was repeated on the same side following an incorrect response to reduce development of side biases. Once rats reached a criterion of 80% correct choices across a test session for two consecutive sessions, this correction procedure was discontinued and a set of two delays was introduced. The presentation of delay durations was randomized within each block of seven trials, such that each delay was presented once within a block. Upon establishing >80% correct responses across two consecutive sessions in a "delay set", rats were progressed to the next set, which contained increasingly longer delays (delay set 1: 0, 2, 4 s; delay set 2: 0, 2, 4, 8, 12, 18, and 24 s).

2.3. Neurobiological measures

2.3.1. Tissue preparation

At the end of behavioral testing, rats were given a two-week period in which they were returned to *ad libitum* feeding prior to brain extractions. Procedures were done according to our previous work (A. R. Hernandez et al., 2018b, 2018a; C. M. Hernandez et al., 2018). Brain slices containing PrL, NAc, and BLA were prepared from rats a minimum of two weeks after the final operant task. Rats were decapitated, brains were rapidly extracted and frozen in an isopentane bath surrounded with dry ice. Coronal slices (360 μm) containing PrL, NAc, and BLA were prepared using a Cryostat (Leica) at −10C. Tissue punches of each brain region were made using a 1 mm punch tool and transferred to T-Per (Thermo Scientific 78510) homogenization buffer. Samples were homogenized by mechanically disturbing the tissue using a pipette. Protein concentrations were determined with the BCA method.

2.3.2. Multiplex ELISA and Simple Western on JESS

Protein samples were split into two aliquots of at least 100 μL for follow-up protein quantification using ELISA or Simple Western techniques. At least 100 μL of protein from each sample was assessed by multiplex ELISA (Raybiotech) using arrays focused on proteins associated with inflammation (Rat Cytokine Array Q67; see Table 2 for Gene-Protein names and descriptions). The remainder of the protein was used for Simple Western experiments to optimize antibodies targeting amyloid beta (Aβ: 6E10, BioLegend 803001; (Abramowski et al., 2012; Cohen et al., 2013; Forny-Germano et al., 2014; Herzig et al., 2004; Kumar et al., 2016; Miyamoto et al., 2016; Oddo et al., 2005; Thakker et al., 2009), phosphorylated tau (pTau-Tyr18: 9G3 MediMabs MM-0194-P; pTau-Thr231: AT180 Thermo Scientific MN1040; pTau-Ser202-Thr205: AT8, Thermo Scientific MN1020), astrogliosis (GFAP: GA5 Cell Signaling Technology 3670), and microglia activation (Iba1: VWR 100369-764). After antibody optimizations were complete according to the manufacturer's suggestions, all samples were prepared according to the manufacturer's suggested protocol for protein quantification using the 12–230 kDa 25-capillary fluorescent separation module (SM-FL004) and protein normalization module (BioTechne:

Table 2
Protein panel information.

Target	Uniprot	GeneName	GeneID	Description
4-1BB	Q4W8J3	Tnfrsf9	0	4-1BB homolog
Activin A	P18331	Activin A	29200	Inhibin beta A chain (Activin beta-A chain)
Adiponectin	Q8K3R4	Adiponectin	246253	30 kDa adipocyte complement-related protein (Adiponectin, C1Q and collagen domain-containing)
b-NGF	P25427	Beta-NGF	310738	Beta-nerve growth factor (Beta-NGF)
B7-1	Q62624	CD80	0	B7-1
B7-2	O35531	CD86	56822	CD86 molecule (Cd86 antigen, isoform CRA_c) (Membrane glycoprotein)
CD48	P10252	CD48	245962	CD48 antigen (BCM1 surface antigen) (BLAST-1) (MRC OX-45 surface antigen) (SLAM family member 2) (SLAMF2) (Signaling lymphocytic activation molecule 2) (CD antigen CD48)
CINC-1	P14095	CINC1	81503	Growth-regulated alpha protein (C-X-C motif chemokine 1) (Cytokine-induced neutrophil chemoattractant 1) (CINC-1) (Platelet-derived growth factor-inducible protein KC)
CINC-2	Q10746	CINC2	171551	C-X-C motif chemokine 3 (Cytokine-induced neutrophil chemoattractant 2) (CINC-2) (Macrophage inflammatory protein 2-alpha/beta) (MIP2-alpha/beta)
CINC-3	P30348	CINC3	114105	C-X-C motif chemokine 2 (Cytokine-induced neutrophil chemoattractant 3) (CINC-3) (Macrophage inflammatory protein 2) (MIP2)
CNTF	P20294	CNTF	25707	Ciliary neurotrophic factor (CNTF)
CTACK	D4AAL6	CCL27	362505	C–C motif chemokine ligand 27 (Chemokine (C–C motif) ligand 27 (Predicted), isoform CRA_b)
Decorin	Q01129	Decorin	29139	Decorin (Bone proteoglycan II) (Dermatan sulfate proteoglycan-II) (DSPG) (PG-S2) (PG40)
Eotaxin	#N/A	Eotaxin	#N/A	#N/A
EphA5	P54757	EphA5	79208	Ephrin type-A receptor 5 (EC 2.7.10.1) (EPH homology kinase 1) (EHK-1)
Erythropoietin	P29676	Erythropoietin	24335	Erythropoietin
FGF-BP	Q9QY10	FGF-BP	64535	Fibroblast growth factor-binding protein 1 (FGF-BP) (FGF-BP1) (FGF-binding protein

Table 2 (*continued*)

Target	Uniprot	GeneName	GeneID	Description
				1) (FGFBP-1) (Growth factor-binding protein 1)
Flt-3L	#N/A	FLT3LG	#N/A	#N/A
Fractalkine	O55145	Fractalkine	89808	Fractalkine (C-X3-C motif chemokine 1) (CX3C membrane-anchored chemokine) (Neurotactin) (Small-inducible cytokine D1) [Cleaved into: Processed fractalkine]
Galectin-1	P11762	Galectin-1	56646	Galectin-1 (Gal-1) (14 kDa lectin) (Beta-galactoside-binding lectin L-14-I) (Galaptin) (Lactose-binding lectin 1) (Lectin galactoside-binding soluble 1) (RL 14.5) (S-Lac lectin 1)
Galectin-3	P08699	Galectin-3	83781	Galectin-3 (Gal-3) (35 kDa lectin) (Carbohydrate-binding protein 35) (CBP 35) (Galactose-specific lectin 3) (IgE-binding protein) (Laminin-binding protein) (Lectin L-29) (Mac-2 antigen)
Gas 1	M0RBH9	Gas1	683470	Growth arrest-specific 1
GFR alpha-1	Q62997	GFRa1	25454	GDNF family receptor alpha-1 (GDNF receptor alpha-1) (GDNFR-alpha-1) (GFR-alpha-1) (RET ligand 1) (TGF-beta-related neurotrophic factor receptor 1)
GM-CSF	P48750	GMCSF	116630	Granulocyte-macrophage colony-stimulating factor (GM-CSF) (Colony-stimulating factor) (CSF)
gp130	P40190	IL6ST	0	Interleukin-6 receptor subunit beta (IL-6 receptor subunit beta) (IL-6R subunit beta) (IL-6R-beta) (IL-6RB) (Interleukin-6 signal transducer) (Membrane glycoprotein 130) (gp130) (Oncostatin-M receptor subunit alpha) (CD antigen CD130)
HGF	P17945	HGF	24446	Hepatocyte growth factor (Hepatopoietin-A) (Scatter factor) (SF) [Cleaved into: Hepatocyte growth factor alpha chain; Hepatocyte growth factor beta chain]
ICAM-1	Q00238	ICAM1	25464	Intercellular adhesion molecule 1 (ICAM-1) (CD antigen CD54)
IFNg	P01581	IFNg	25712	Interferon gamma (IFN-gamma)
IL-1 R6	Q62929	IL1rL2	171106	Interleukin-1 receptor-like 2 (IL-36 receptor) (Interleukin-1

(continued on next page)

Table 2 (*continued*)

Target	Uniprot	GeneName	GeneID	Description
				receptor-related protein 2) (IL-1Rrp2) (IL1R-rp2)
IL-1 ra	#N/A	IL1r1	#N/A	#N/A
IL-10	P29456	IL10	25325	Interleukin-10 (IL-10) (Cytokine synthesis inhibitory factor) (CSIF)
IL-13	P42203	IL13	116553	Interleukin-13 (IL-13) (T-cell activation protein P600)
IL-17F	Q5BJ95	IL17F	301291	Interleukin-17F (IL-17F)
IL-1a	P16598	IL1a	24493	Interleukin-1 alpha (IL-1 alpha)
IL-1b	Q63264	IL1b	0	Interleukin-1 beta (IL-1 beta)
IL-2	P17108	IL2	116562	Interleukin-2 (IL-2) (T-cell growth factor) (TCGF)
IL-2 Ra	P26897	IL2ra	25704	Interleukin-2 receptor subunit alpha (IL-2 receptor subunit alpha) (IL-2-RA) (IL-2R subunit alpha) (IL2-RA) (CD antigen CD25)
IL-22	G3V6X6	IL22	500836	Interleukin 22 (Similar to TIF alpha protein (Predicted))
IL-3	P04823	IL3	0	Interleukin-3 (IL-3) (Hematopoietic growth factor) (Mast cell growth factor) (MCGF) (Multipotential colony-stimulating factor) (P-cell-stimulating factor)
IL-4	P20096	IL4	287287	Interleukin-4 (IL-4) (B-cell IGG differentiation factor) (B-cell growth factor 1) (B-cell stimulatory factor 1) (BSF-1) (Lymphocyte stimulatory factor 1)
IL-6	P20607	IL6	24498	Interleukin-6 (IL-6)
IL-7	P56478	IL7	0	Interleukin-7 (IL-7)
JAM-A	Q9JHY1	JAM-A	116479	Junctional adhesion molecule A (JAM-A) (Junctional adhesion molecule 1) (JAM-1) (CD antigen CD321)
L-Selectin	P30836	L-Selectin	0	L-selectin (CD62 antigen-like family member L) (Leukocyte adhesion molecule 1) (LAM-1) (Leukocyte-endothelial cell adhesion molecule 1) (LECAM1) (Lymph node homing receptor) (Lymphocyte antigen 22) (Ly-22) (Lymphocyte surface MEL-14 antigen) (CD antigen CD62L)
LIX	P97885	CXCL5	60665	C-X-C motif chemokine 5 (Cytokine LIX) (Small-inducible cytokine B5)
MCP-1	P14844	MCP1	24770	C–C motif chemokine 2 (Immediate-early serum-responsive protein JE) (Monocyte

Table 2 (*continued*)

Target	Uniprot	GeneName	GeneID	Description
				chemoattractant protein 1) (Monocyte chemotactic protein 1) (MCP-1) (Small-inducible cytokine A2)
MIP-1a	P50229	MIP1a	25542	C–C motif chemokine 3 (Macrophage inflammatory protein 1-alpha) (MIP-1-alpha) (Small-inducible cytokine A3)
Neuropilin-1	Q9QWJ9	Neuropilin-1	246331	Neuropilin-1 (Vascular endothelial cell growth factor 165 receptor) (CD antigen CD304)
Neuropilin-2	O35276	Neuropilin-2	81527	Neuropilin-2 (Vascular endothelial cell growth factor 165 receptor 2)
Nope	B5DFA9	Nope	0	Nope protein (Fragment)
Notch-1	Q07008	Notch1	25496	Neurogenic locus notch homolog protein 1 (Notch 1) [Cleaved into: Notch 1 extracellular truncation (NEXT; Notch 1 intracellular domain (NICD)]
Notch-2	Q9QW30	Notch2	0	Neurogenic locus notch homolog protein 2 (Notch 2) [Cleaved into: Notch 2 extracellular truncation; Notch 2 intracellular domain]
P-Cadherin	F1LMI3	P-Cadherin	116777	Cadherin 3, type 1, P-cadherin (Placental)
PDGF-AA	P28576	PDGFA	25266	Platelet-derived growth factor subunit A (PDGF subunit A) (PDGF-1) (Platelet-derived growth factor A chain) (Platelet-derived growth factor alpha polypeptide)
Prolactin	P01237	Prolactin	24683	Prolactin (PRL)
Prolactin R	P05710	PRLR	24684	Prolactin receptor (PRL-R) (Lactogen receptor)
RAGE	Q63495	RAGE	0	Advanced glycosylation end product-specific receptor (Receptor for advanced glycosylation end products)
RANTES	P50231	RANTES	0	C–C motif chemokine 5 (SIS-delta) (Small-inducible cytokine A5) (T-cell-specific protein RANTES)
SCF	P21581	SCF	60427	Kit ligand (Hematopoietic growth factor KL) (Mast cell growth factor) (MGF) (Stem cell factor) (SCF) (c-Kit ligand) [Cleaved into: Soluble KIT ligand (sKITLG)]
TCK-1	Q99ME0	CXCL7	246358	CXC chemokine RTCK1 (Chemokine (C-X-C motif) ligand 7,

Table 2 (*continued*)

Target	Uniprot	GeneName	GeneID	Description
TIM-1	O54947	TIM1	286934	isoform CRA_b) (Pro-platelet basic protein) Hepatitis A virus cellular receptor 1 homolog (HAVcr-1) (Kidney injury molecule 1) (KIM-1) (T cell immunoglobulin and mucin domain-containing protein 1) (TIMD-1)
TIMP-1	P30120	TIMP1	116510	Metalloproteinase inhibitor 1 (Tissue inhibitor of metalloproteinases 1) (TIMP-1)
TIMP-2	P30121	TIMP2	29543	Metalloproteinase inhibitor 2 (Tissue inhibitor of metalloproteinases 2) (TIMP-2)
TNFa	P16599	TNFa	24835	Tumor necrosis factor (Cachectin) (TNF-alpha) (Tumor necrosis factor ligand superfamily member 2) (TNF-a) [Cleaved into: Tumor necrosis factor, membrane form (N-terminal fragment) (NTF); Intracellular domain 1 (ICD1); Intracellular domain 2 (ICD2); C-domain 1; C-domain 2; Tumor necrosis factor, soluble form]
TREM-1	D4ABU7	TREM1	301229	Triggering receptor-expressed on myeloid cells 1
TWEAK R	Q80XX9	Tnfrsf12a	302965	Tumor necrosis factor receptor superfamily, member 12a (Type 1 transmembrane protein FN14)
VEGF	#N/A	VEGF	#N/A	#N/A

DM-PN02). Specifically, each animal served as a biological replicate, and as such, there was n = 14 WT and n = 14 TgAD samples loaded across two separation modules. Samples with technical errors such as discrepancies with total protein loaded were rerun. Electropherograms were used to quantify peaks at expected molecular weights as validated by previously published studies. Specifically, Aβ (6E10) was validated by the manufacturer's website showing bands at <10 kDa and at ~130 kDa; pTau-Tyr18 (9G3) was validated by the manufacturer and by Dourlen and colleagues showing doublet bands between 50 and 64 kDa (Dourlen et al., 2017); pTau-Thr231 (AT180) was validated by the manufacturer and by Nies and colleagues showing doublet bands between 50 and 64 kDa (Nies et al., 2021); pTau-Ser202-Thr205 (AT8) was also validated by the manufacturer and by Dourlen and colleagues showing triplet or doublet bands between 50 and 64 kDa (Dourlen et al., 2017); GFAP (GA5) was validated by the manufacturer showing a band at ~50 kDa; and Iba1 was validated by the manufacturer showing a band at ~20 kDa. All protein targets were measured in the chemiluminescence channel whereas total protein quantification was measured in the fluorescence channel according to the manufacturer's suggestion.

2.4. Statistical analysis and experimental design

2.4.1. General statistical approach

Unless otherwise noted, all statistical analyses were performed in SPPSS28 v280.0.0(190). In all analyses, the alpha (α) was set to 0.05, and when Mauchly's test of sphericity was violated, the Huynh-Feldt p-value correction was applied. When there were significant effects, the effect sizes were reported as η_p^2 for ANOVAs and Cohen's d for t-tests. Additionally, observed power for significant effects was reported as 1-β. For brevity, all null effects were reported as consolidated F- or t-statistics, p-values, and only the lowest and highest values for each were given. Behavioral outliers were identified using the outlier identification analysis in SPSS. In all analyses, genotype and sex were coded as nominal variables and any repeated measure was coded as continuous. All figures were generated in GraphPad Prism v10.10(264).

2.4.2. Evaluation of intertemporal choice

Percent choice of the large, delayed reward and free choice trial omissions were analyzed using a mixed-factor ANOVA (genotype × sex × delay) with genotype (2 levels: WT and TgAD) and sex (2 levels: male and female) as between-subjects factors, and delay (5 levels 0, 10, 20, 40, and 60 s) as the within-subjects factors. Any main effects and interactions between genotype and sex were followed up with pairwise comparisons using Fishers Least Significant Difference (LSD). Significant pairwise comparisons were reported as mean difference followed by p-values. Total rewards earned were compared using a mixed-factor ANOVA (genotype × sex).

2.4.3. Evaluation of food motivation in intertemporal choice

To determine if genotype differences in choice performance were due to differences in motivation to obtain food under food restriction conditions, rats were tested in the intertemporal choice task following both a 1-h *ad libitum* feeding schedule. To counterbalance testing, half of WT and TgAD rats in the cohort were placed on a 1-h *ad libitum* feeding schedule prior to testing on the intertemporal choice task on the first day. On the following day, all rats were tested under the usual food-restricted conditions (as a "washout period" for the 1-h *ad libitum* feeding schedule). On the third day, the second half of the cohort was given the 1-h *ad libitum* feeding schedule. Comparisons of choice performance under the *ad libitum* feeding conditions were conducted using a four-factor, mixed-factor ANOVA, with genotype and sex as the between-subjects factors and both feeding condition (*ad libitum* vs. food-restricted) and delay as within-subjects factors. Free-choice trial omissions were compared using a mixed-factor, repeated-measures ANOVA with genotype and sex as a between-subjects factors and feeding condition and delay as a within-subjects factors.

2.4.4. Evaluation of delay and reward magnitude discrimination

To determine if genotype differences in choice performance were due to differences in delay or reward discrimination, rats were tested in the intertemporal choice task under delay- or reward-modified conditions. To evaluate delay perception (or discrimination) differences, all rats progressed through a modified intertemporal choice task in which both levers delivered a small reward (1 food pellet) at increasing delays across trial blocks. Data were analyzed using a mixed-factor ANOVA (genotype × sex × delay). To evaluate reward magnitude discrimination differences, a subset of rats (n = 6 WT and n = 6 TgAD) progressed through 5 additional days of testing in which the large, delayed reward was 3 pellets and an additional 5 days of testing in which the large, delayed reward was 2 pellets. Data for all reward schedules were averaged across blocks and analyzed using a mixed-factor ANOVA (genotype × reward magnitude) with genotype the between-subjects factor and reward magnitude as the within-subjects factor (sex was underpowered and thus omitted as a factor). Finally, the total rewards earned were compared across reward schedules using the same design.

2.4.5. Evaluation of progressive ratio

The break points (last completed schedule), total number of lever presses, and activity per session on the progressive ratio task were used as measures of performance. These measures were analyzed using a mixed-factor ANOVA (genotype $\times$ sex $\times$ reward magnitude). Values (breakpoint, total lever presses, and activity) for the 1-pellet reward were averaged across the final three test sessions to provide a mean value for each rat, whereas the 4-pellet reward was a singular test session on the final day of progressive ratio testing.

2.4.6. Evaluation of set shifting

The total numbers of trials to criterion (10 consecutive trials) and errors required to achieve criterion performance on the visual discrimination and set shift were the primary measures of performance. In addition, errors during the set shift were subdivided into those that were previously reinforced (i.e., errors attributable to perseveration on the previously learned rule) and those that were never-reinforced (i.e., errors that were inconsistent with both the initial rule and the rule following the set shift). Trials to criterion during visual discrimination and set-shift were analyzed using a mixed-factor ANOVA (genotype $\times$ sex). Errors were analyzed using a mixed-factor ANOVA (genotype $\times$ sex $\times$ error type).

2.4.7. Evaluation of delayed match-to-sample

Accuracy (percent correct at each delay) was the primary measure of delayed response performance (Bañuelos et al., 2014; Beas et al., 2013). Upon reaching delay set 2, performance accuracy (% correct) was evaluated across the last three days of an 8-day training period. Performance at each delay was averaged across these 3 sessions, and comparisons were conducted using a mixed-factor ANOVA genotype $\times$ sex $\times$ delay), with delay (7 levels: 0, 2, 4, 8, 12, 18, 24 s) as a within-subjects factor. Latency to respond during the matching phase was also assessed in the same 3 sessions. Latency to respond during the choice phase was calculated separately for correct and incorrect trials (averaged across all delays). Latency data were analyzed using a multi-factor ANOVA, with genotype and sex as between-subjects factors, and matching outcome (2 levels, correct vs. incorrect) as a within-subjects factor. Finally, the number of trials completed per session was monitored and compared between ages using a two-factor ANOVA (genotype $\times$ sex).

2.4.8. Evaluation of relationships between behavioral performances

A principal components analysis (PCA) was used to analyze associations between performance on each task. The measures loaded included percent choice of the large, delayed rewards average across 10–60 s (intertemporal choice), total lever presses under a 4-pellet reward condition (progressive ratio), trials to criterion during the set-shift (set-shift), and percent correct averaged across 18–24 s (delayed match-to-sample). The rotation used was Varimax with Kaiser normalization. The Scree method was used to determine the solution. Component scores were extracted as regression loadings. To determine group differences, regression loadings were analyzed using a multivariate ANOVA with genotype and sex the fixed factors (DiStefano et al., 2009).

2.4.9. Evaluation of associations between markers of inflammation and behavioral performance

Employing a modified version of an analysis pipeline used by Elkhatib and colleagues in 2020 (Elkhatib et al., 2020), we used a PCA to reduce the dimensionality of the results from multiplex ELISA measurements. Data from each protein sample measured per region was loaded into a PCA. Brain regions were analyzed separately. The rotation used was Varimax with Kaiser normalization. The Scree method was used to determine the solution, or number of meaningful components. Component scores were extracted as regression loadings. Each component represented a cluster of proteins. To determine group differences, regression loadings for each component (cluster) were analyzed using a multivariate ANOVA with genotype and sex as fixed factors (DiStefano et al., 2009). Proteins contributing to their respective clusters were further analyzed using Gene Ontology Bioinformatics via CytoScape (v3.10.1) to determine GO terms for each cluster. Clusters were further analyzed with CytoScape (v3.10.1) to determine protein-protein interaction networks. Finally, PCA cluster data was validated with a weighted correlation network analysis using clustergrammer (Fernandez et al., 2017).

2.4.10. Evaluation of proteins associated with pathology and gliosis and their influence on markers of inflammation and behavioral performance

Data from Simple Western JESS runs were extracted using Compass Software for Simple Western (v6.3.0). Raw data (area under the curve) from electropherogram peaks at expected molecular weights were normalized to total protein loaded. To place all the within the same scale for presentation purposes, Z-scores were plotted. Data were compared using a two-factor ANOVA (genotype $\times$ sex).

3. Results

3.1. Maladaptive intertemporal choice decision strategy in young adult TgAD rats

Prior to the end of behavioral testing, a total of n = 5 rats were removed. Two rats (n = 1 WT and n = 1 TgAD) failed to complete behavioral shaping, and 3 rats (n = 2 WT and n = 1 TgAD) were behavioral outliers. Because of the focus on individual variability between behavior and pathology, outliers were removed for the entire study. As such, final group numbers were n = 14 WT and n = 14 TgAD (Table 1). Rats were 6.48 months old at the beginning of behavioral shaping, and the duration of behavioral shaping was 0.57 months. Notably, a univariate ANOVA confirmed there were no group differences in the number of sessions it took to learn the behavioral shaping contingencies ($Fs_{(1,24)} = 0.022$–2.155; ps = 0.155–0.884; Means $\pm$ S.E. M.: WT males = 15.667 $\pm$ 3.914, females = 20.50 $\pm$ 3.390; TgAD males = 16.750 $\pm$ 3.390, females = 22.667 $\pm$ 22.667).

The decision-making process requires intact executive function and emotional affect. AD is associated with perturbations in cognitive domains including decision making. To determine if young adult TgAD rats demonstrate cognitive and emotional affect dysfunction, we tested them on the intertemporal choice task (Fig. 1A). On average, rats were 7.2 months old at the beginning of intertemporal choice testing, and the duration of testing was 0.8 months. All rats decreased their preference for the large reward as the delay increased (delay: $F_{(4,96)} = 47.540$; p < 0.001; $\eta^2 = 0.665$; 1-β = 1.000; Fig. 1B). Relative to WT young adults, TgAD rats maintained a greater preference for the large, delayed reward (genotype: $F_{(1,24)} = 11.396$; p = 0.003; $\eta^2 = 0.322$; 1-β = 0.899) as the delay to reward increased (genotype $\times$ delay: $F_{(4,96)} = 6.734$; p < 0.001; $\eta^2 = 0.219$; 1-β = 0.954; Fig. 1B and C). There were no effects of sex or interactions with sex ($Fs_{(1-4,24-96)} = 0.212$–0.985; ps = 0.398–0.808). This effect was not due to procedural differences as there were no differences in percent choice of the large reward under no delay condition (WT = 98.681 vs TgAD = 100.00; $F_{(1,24)} = 2.408$, p = 0.134; Fig. 1B).

We then tested whether greater preference of large, delayed rewards in TgAD rats translated into a greater number of rewards earned, as would be the case if greater choice of large, delayed rewards was a strategy for maximizing overall reward yield. Relative to WT young adults, TgAD rats did not have a greater number of rewards earned ($t_{(26)} = -1.286$, p = 0.210; Fig. 1D). To further investigate this result, we analyzed the number of trial omissions per delay block. All rats omitted more trials at longer delays relative to shorter delays ($F_{(4,104)} = 37.722$, p < 0.001; $\eta^2 = 0.592$, 1-β = 1.000; Fig. 1E). However, TgAD rats omitted a significantly greater number of trials relative to WT (genotype: $F_{(1,26)} = 6.562$, p = 0.017, $\eta^2 = 0.202$, 1-β = 0.684; Fig. 1E), and this effect trended towards occurring more at longer delays ($F_{(4,104)} = 2.367$, p = 0.094, $\eta^2 = 0.083$, 1-β = 0.501; Fig. 1E). Finally, we tested

whether rats would have gained significantly more rewards given they completed all trials at their measured choice preference. That is, was TgAD and WT rats' predicted number of rewards greater than their actual earned rewards. Indeed, a paired samples *t*-test confirmed rats' predicted rewards were greater in TgAD ($t_{(13)}$ = -6.789, p < 0.001; Fig. 1D) and WT rats ($t_{(13)}$ = -4.274, p < 0.001; Fig. 1D), with the mean difference in actual vs predicted rewards earned in TgAD rats being greater than the mean difference in WT rats (TgAD: 35.45; WT: 15.74). Notably, TgAD rats would have earned significantly more rewards relative to WT if they completed all possible trials ($t_{(26)}$ = -3.442, p = 0.002; Fig. 1D), and the mean difference between WT and TgAD in actual vs predicted was 32 rewards, thus confirming a maladaptive decision strategy. Together, these results suggest while TgAD rats choose the large reward more than the WT rats, their choices do not translate into a greater reward yield suggesting an impairment in decision-making strategy given the objective to maximize reward gains (reward maximization forfeiture).

To determine if any genotype effects were hunger state dependent, we implemented a 24-hr *ad libitum* feeding schedule after intertemporal choice testing was complete. On day one, half the rats received 24 h of *ad libitum* feeding while the other half remained on a food restricted feeding schedule. The following day, all rats were tested, and the feeding schedule was reversed immediately after testing such that the other half of the rats received 24 h ad libitum feeding while the other half were placed back on a food-restricted schedule. Consistent with group differences on intertemporal choice, there were effects of delay ($F_{(4,104)}$ = 41.837, p < 0.001, η^2 = 0.617, 1-β = 1.000; Supplementary Fig. 1A), genotype ($F_{(1,26)}$ = 4.531, p = 0.043, η^2 = 0.148, 1-β = 0.536), and a genotype by delay interaction ($F_{(4,104)}$ = 3.159, p = 0.021, η^2 = 0.108, 1-β = 0.776). However, there were no main effects of feeding schedule ($F_{(1,26)}$ = 0.342, p = 0.564; Supplementary Fig. 1A), nor any interactions of feeding schedule with genotype ($Fs_{(1-4,26-104)}$ = 0.123–0.539, ps = 0.671–0.729). We did follow up a significant interaction between feeding schedule and delay irrespective of genotype ($F_{(4,104)}$ = 2.748, p = 0.044, η^2 = 0.096, 1-β = 0.670) and confirmed percent choice at most delays did not significantly differ between feeding schedules ($Fs_{(1,26)}$ = 0.583–2.712, ps = 0.112–0.452) except for a trend at the 20 s delay such that *ad libitum* decreased choice of the large reward from 64.663% to 50.982% ($F_{(1,26)}$ = 3.314, p = 0.080, η^2 = 0.113, 1-β = 0.418). Importantly, this effect was irrespective of genotype.

As a measure of ensuring the *ad libitum* feeding schedule was effective, we tested whether rats were generally more satiated by comparing trial omissions between feeding schedules during their free choice trials. All rats increased trial omissions under the *ad libitum* feeding schedule irrespective of genotype ($F_{(1,26)}$ = 42.002, p < 0.001, η^2 = 0.618, 1-β = 1.000; Supplementary Fig. 1B) suggesting all rats were equally satiated, and this effect was largest as delays increased (delays: $F_{(4,104)}$ = 21.706, p < 0.001, η^2 = 0.455, 1-β = 1.000; feeding schedule × delay: $F_{(4,104)}$ = 2.195, p = 0.025, η^2 = 0.101, 1-β = 0.768). As expected, TgAD omitted more trials relative to WT rats (genotype: $F_{(1,26)}$ = 6.854, p = 0.015, η^2 = 0.209, 1-β = 0.712; genotype × feeding schedule × delay: $F_{(4,104)}$ = 3.289, p = 0.014, η^2 = 0.112, 1-β = 0.823). There were no other effects ($Fs_{(1-4,26-104)}$ = 0.136–1.964, ps = 0.173–0.947).

We then asked if differences in choice performance could be explained by differences in delay perception. That is, increased preferences for large, delayed rewards in TgAD rats could be due to longer delays being perceived similarly to short delays. To test this hypothesis, we equated the ratio of immediate and delayed rewards to one food pellet (1:1, immediate to delayed rewards) and maintained the same increasing delays per block. While there was a main effect of delay ($F_{(4,104)}$ = 169.515, p < 0.001, η^2 = 0.867, 1-β = 1.000; Supplementary Fig. 1C), there were no effects of, or interactions with, genotype ($Fs_{(1-4,26-104)}$ = 0.651–1.041, ps = 0.360–0.427). These results suggest differences between WT and TgAD rats are not due to differences in delay perception.

We also asked if differences in choice of large, delayed reward would

persist under decreasing ratios between the large and small rewards (i.e., 4:1, 3:1, and 2:1). In a subset of rats (n = 6 WT and n = 6 TgAD), we reduced the ratio of delayed to immediate rewards from 4:1 to 3:1 to 2:1. We used the average of 0–60s to test if group differences persisted. All rats decreased their preference for the large delayed reward as the ratio decreased ($F_{(2,20)}$ = 83.282, p < 0.001, η^2 = 0.893, 1-β = 1.000; Supplementary Fig. 1D). Importantly, TgAD rats maintained a greater preference for the large, delayed reward at each ratio relative to WT (genotype: $F_{(1,10)}$ = 11.143, p = 0.008, η^2 = 0.527, 1-β = 0.852; genotype × reward ratio: $F_{(2,20)}$ = 4.286, p = 0.028, η^2 = 0.300, 1-β = 0.679). Expectedly, all rats decreased their total number of rewards earned as the reward ratio decreased ($F_{(2,20)}$ = 50.331, p < 0.001, η^2 = 0.834, 1-β = 1.000). Despite their greater preference for the large, delayed reward at each ratio, TgAD rats did not significantly earn a greater number of rewards at any ratio ($Fs_{(1-2,10-20)}$ = 0.303–3.750, ps = 0.082–0.742; Supplementary Fig. 1E). However, in this subset of rats, there was a weak trend in the main effect of genotype irrespective of reward ratio driven by a relatively small numerical difference of 14.9 rewards ($F_{(1,10)}$ = 3.750, p = 0.082, η^2 = 0.273, 1-β = 0.417).

3.2. Motivational deficits in young adult TgAD rats

To test if TgAD rats' compromised decision strategy (i.e., forfeiture to maximize rewards) could be explained by increase apathy (or lack of motivation), all rats were tested on a progress ratio task with two reward magnitude schedules (1-pellet then 4-pellet; Fig. 2A). On average, rats were 8.53 months old at the beginning of progressive ratio testing, and the duration of testing was 0.07 months. All rats demonstrated an increase in lever presses when moved to a 4-pellet schedule from a 1-pellet schedule ($F_{(1,24)}$ = 15.258; p < 0.001; η^2 = 0.389; 1-β = 0.963; Fig. 2B). Relative to WT young adults, TgAD rats performed significantly lower lever presses (genotype: $F_{(1,24)}$ = 7.387; p = 0.012; η^2 = 0.235; 1-β = 0.741), specifically when the reward was 4-pellets (genotype × reward magnitude: $F_{(1,24)}$ = 12.498; p = 0.002; η^2 = 0.342; 1-β = 0.924). Interestingly, there was also a sex difference such that all females performed a greater number of lever presses relative to males (sex: $F_{(1,24)}$ = 5.653; p = 0.026; η^2 = 0.191; 1-β = 0.626; Fig. 2C). Sex also interacted with genotype and reward magnitude (genotype × reward magnitude × sex: $F_{(1,24)}$ = 5.346; p = 0.030; η^2 = 0.182; 1-β = 0.602). Follow up simple main effects on estimated marginal means confirmed while WT males performed more than double the lever presses relative to TgAD males, this result was not significant (92.167 presses for 1 pellet in Male WT vs 41.708 presses for 1 pellet in Male TgAD, $F_{(1,24)}$ = 1.219, p = 0.281; 128.500 presses for 4 pellets in Male WT vs 50.375 presses for 4 pellets in Male TgAD, $F_{(1,24)}$ = 1.247, p = 0.275). Relative to WT females, TgAD female rats performed a significantly lower number of lever presses, specifically under a 4-pellet schedule (185.000 presses for 1 pellet in Female WT vs 96.778 presses for 1 pellet in Female TgAD, $F_{(1,24)}$ = 3.726, p = 0.065; 317.000 presses for 4 pellets in Female WT vs 96.500 presses for 4 pellets in Female TgAD, $F_{(1,24)}$ = 9.934, p = 0.004).

We then asked if these effects were due to differences in general activity. While all rats increased their activity during the 4-pellet schedule relative to the 1-pellet schedule (reward magnitude: $F_{(1,24)}$ = 4.938, p = 0.036, η^2 = 0.171, 1-β = 0.569), there was no main effect of genotype (genotype: $F_{(1,24)}$ = 1.276, p = 0.270; Fig. 3D) or sex (sex: $F_{(1,24)}$ = 1.018, p = 0.323). Though there were no other effects ($Fs_{(1,24)}$ = 0.125–1.276, ps = 0.270–0.727), there was a trending genotype × reward magnitude interaction ($F_{(1,24)}$ = 3.713, p = 0.066, η^2 = 0.134, 1-β = 0.456). However, when testing simple main effects, there were no genotype differences in activity under the 1-pellet reward magnitude schedule ($F_{(1,24)}$ = 0.241, p = 0.628) or the 4-pellet reward magnitude schedule ($F_{(1,24)}$ = 2.359, p = 0.138). Together, these results suggest decreased motivation in TgAD young adults relative to WT rats, and this decreased motivation may be driven by young adult female TgAD rats.

A. Progressive Ratio Task

Fixed Ratios (FRs) Progressively Increase
1 Lever press=1 Reward→3 Lever presses=1 Reward, etc.

| 1 | 3 | 6 | 10 | 15 | 20 | 25 | 32 | ... | 355 |

B.

D.

C.
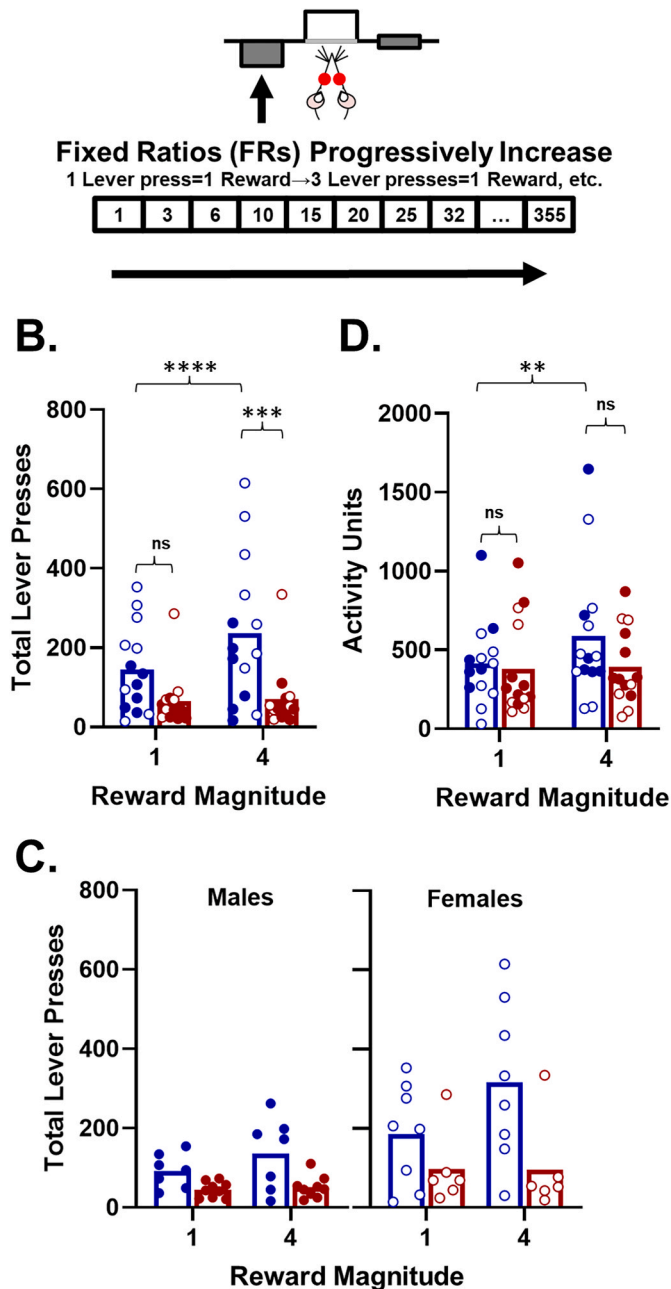
Fig. 2. Progressive ratio. A. Schematic of progressive ratio task. **B.** Though there was no statistical difference between TgAD and WT rats in the number of lever presses to obtain 1 food pellet reward, TgAD rats preformed significantly less lever pressed than the WT rats when the food reward was 4 pellets. Moreover, WT rats expectedly increased there number of lever presses for the 4-pellet food reward relative to the 1-pellet food rewards, whereas TgAD rats did not. D. Group differences were not due to differences in overall activity or motoric deficits. **C.** When stratified by sex, male TgAD rats numerically performed less lever presses for both rewards, though it was statistically significant. In contrast, female TgAD rats performed significantly fewer lever presses relative to female WT rats for both rewards. In all panels, **p < 0.01, ***p < 0.001, ****p < 0.001, and ns = not significant; blue represents WT rats, and red represents TgAD rats. Animal numbers in this experiment were n = 14 WT (n = 8 females, n = 6 males) and n = 14 TgAD (n = 6 females, n = 8 males). Females are represented by open circles and males are represented by closed circles. (For interpretation of the references to color in this figure legend, the reader is referred to the Web version of this article.)

3.3. Preserved cognitive flexibility in young adult TgAD rats

Decision making requires intact executive function. One of those functions is cognitive flexibility. As such, we then asked if young adult TgAD rats were impaired in a set shifting task that measures medial prefrontal cortical-dependent cognitive flexibility (Fig. 3A). On average, rats were 8.68 months old at the beginning of set-shift (lever bias) testing, and the duration of testing was 0.14 months. There were no group differences in the trials to criterion on the visual discrimination portion of the set-shift task ($Fs_{(1,24)} = 0.022$–1.331, $ps = 0.260$–0.884; Fig. 3B). Additionally, there were no group differences during the set shift (lever location) portion of the task ($Fs_{(1,24)} = 0.056$–0.155, $ps = 0.698$–0.815; Fig. 3C). We considered if there may have been differences in the type of specific errors made (reenforced vs non-reenforced), and while all rats made significantly more reenforced errors than non-reenforced errors ($F_{(1,24)} = 63.986$, $p < 0.001$; Fig. 3D), there were no group differences within error types ($Fs_{(1,24)} = 0.017$–1.269, $ps = 0.271$–0.898). These results suggest that during young adulthood, TgAD rats have spared cognitive flexibility.

3.4. Impaired working memory in young adult TgAD rats

One other executive function critical to decision making is working memory. As such, we asked if working memory was impaired in young adult TgAD rats relative to young adult WT rats (Fig. 4A). On average, rats were 8.97 months old at the beginning of delayed match-to-sample testing, and the duration of testing was 0.45 months. As expected, all rats performed worse as the delay increased ($F_{(6,144)} = 165.943$, $p < 0.001$, $\eta^2 = 0.874$, 1-$\beta = 1.000$; Fig. 4B). However, relative to WT, performance was worse in TgAD rats ($F_{(1,24)} = 5.144$, $p = 0.033$, $\eta^2 = 0.176$, 1-$\beta = 0.586$) and this effect was larger at longer delays ($F_{(6,144)} = 2.861$, $p = 0.022$, $\eta^2 = 0.106$, 1-$\beta = 0.795$; Fig. 4B and C). There was a trending main effect of sex such that females performed better than males irrespective of genotype or delay ($F_{(1,24)} = 4.085$, $p = 0.055$, $\eta^2 = 0.145$, 1-$\beta = 0.492$). There were no other differences in working memory performance ($Fs_{(1,24)} = 0.022$–1.331, $ps = 0.260$–0.884).

We then asked if any differences in working memory performance were due to general task engagement. Genotypic differences were not due to differences in number of trials performed ($t_{(26)} = 1.599$, $p = 0.122$; Fig. 4D). Response latency during the matching phase of the task may be indicative of choice certainty (i.e., faster responses with correct choices). As such, we analyzed the lever response latency during the matching phase. While there were no genotype effects ($Fs_{(1,26)} = 0.007$–0.815, $ps = 0.375$–0.934), all rats took longer to respond when they chose incorrectly ($F_{(1,26)} = 12.505$, $p = 0.002$, $\eta^2 = 0.325$, 1-$\beta = 0.925$; Fig. 4E). Together, these results suggest an early impairment in working memory performance in young adult TgAD rats.

3.5. Rats with greater choice of large, delayed rewards have motivational deficits and impaired working memory

As executive functions (working memory and cognitive flexibility) and emotional affect (motivation) are necessary in the decision-making process, we then asked if there were relationships between performance on all behavioral measures. A PCA reduced the dimensionality of the data from 4 to 2 (2 components extracted) in n = 28 rats to determine associations between performances on intertemporal choice, progressive ratio, set-shifting, and delayed match-to-sample tasks. The eigenvalue pertaining to component 1 was 1.829, and the eigenvalue pertaining to component 2 was 1.099, whereas component eigenvalues were below 0.698 for components 3 and 4.

Component 1 explained 45.719% of the variance whereas component 2 explained 27.479% of the variance, and the cumulative variance was 73.199% (Fig. 5A). Strong loadings on component 1 included intertemporal choice (−0.722), progressive ratio (0.743), and delayed match-to-sample task performance (0.865), whereas set-shifting
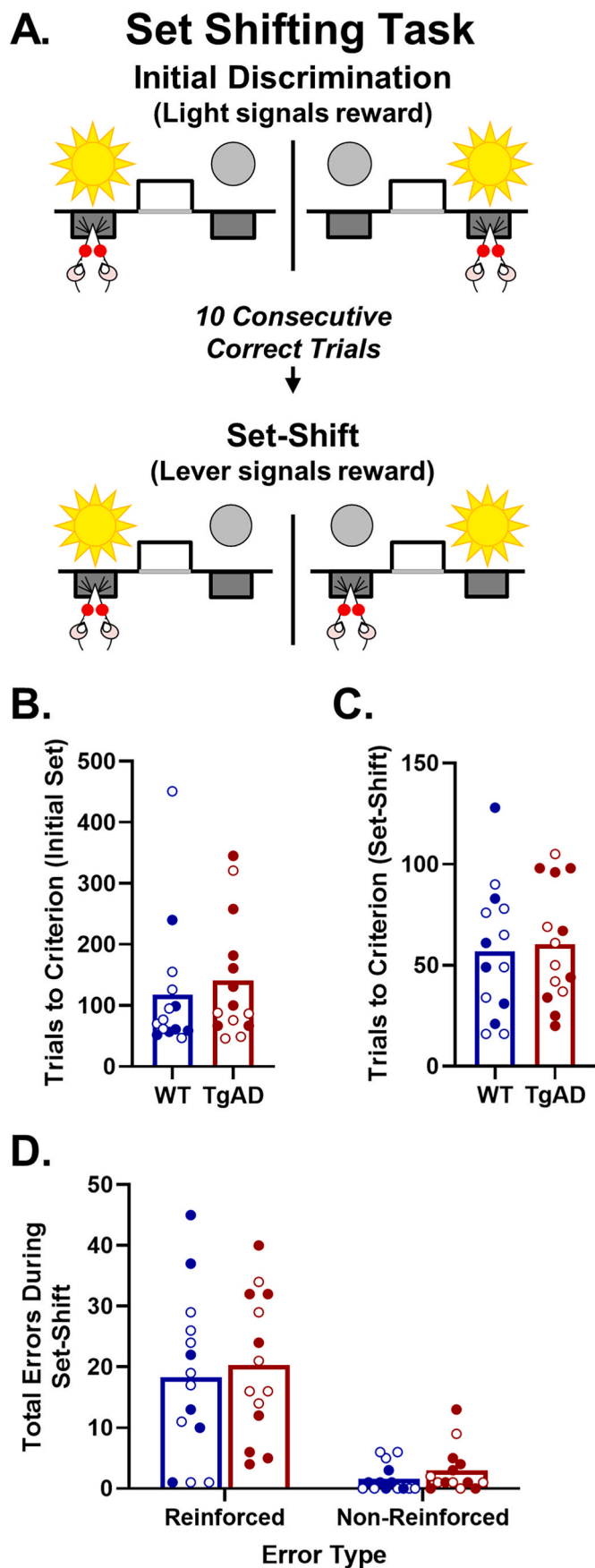
Fig. 3. Set-shifting task of cognitive flexibility. A. Task schematic for the set-shift task. **B.** No group differences in the number of trials to reach criterion for the initial discrimination rule (visual discrimination). **C.** No group differences in the number of trials to criterion during the set-shift (shift to lever rule). These data also suggest group differences in intertemporal choice were not due to cognitive inflexibility. **D.** No group differences in the number or type of errors committed during the set shift. Animal numbers in this experiment were n = 14 WT (n = 8 females, n = 6 males) and n = 14 TgAD (n = 6 females, n = 8 males). Females are represented by open circles and males are represented by closed circles.

performance loaded onto component 2 (0.954). A multivariate analysis on regression scores for component 1 confirmed a main effect of genotype such that TgAD rats significantly clustered more negatively onto component 1 relative to WT rats ($F_{(1,24)} = 10.144$, $p < 0.001$, $\eta^2 = 0.467$, $1\text{-}\beta = 0.993$; Fig. 5B). These data suggested rats with greater choice of large, delayed rewards also had a smaller number of lever presses during progressive ratio responding and worse accuracy during delayed match-to-sample performance, and these rats were predominantly young adult TgAD rats (Fig. 5C, whereas Fig. 5D shows set shift performance loadings). While there was a trending sex effect suggesting females clustered more positively relative to males ($F_{(1,24)} = 3.387$, $p = 0.078$, $\eta^2 = 0.124$, $1\text{-}\beta = 0.423$), there was a significant interaction between genotype and sex ($F_{(1,24)} = 4.626$, $p = 0.042$, $\eta^2 = 0.162$, $1\text{-}\beta = 0.542$). Pairwise comparisons on simple main effects indicated that group differences were larger in females. As such, the genotype effects on intertemporal choice, progressive ratio, and delayed match-to-sample, though driven by all TgAD rats, were more strongly driven by young adult female TgAD rats. In contrast, there were no effects for component 2 ($Fs_{(1,24)} = 0.036\text{-}0.696$, $ps = 0.412\text{-}0.851$).

3.6. Associations between behavioral performance and brain measures of inflammation and pathology

Decision making and executive function are supported by a broad network of cortical and subcortical structures including the PrL, BLA, and NAc. To determine if markers of inflammation significantly clustered by genotype in a region-specific manner, we first used a weighted correlation cluster analysis for proteins assessed via multiplex ELISA. To extract regression scores and test genotypic differences within clusters, we then loaded a PCA with protein measures. Individual protein values per rat are given in Supplementary Tables S1–S3. Furthermore, amyloid pathology, phosphorylated tau, and measures of inflammation or gliosis have yet to be measured in the PrL, BLA, and NAc of young adult TgAD rats. Therefore, we assessed the expression of amyloid plaques, three pTau phospho-sites, GFAP, and Iba1 in these brain structures using a Simple Western technique. On average, rats were 9.4 months old at the time of sacrifice for analyses cytokines, chemokines, immunotropic factors, and AD-like pathology in region-specific brain tissue.

3.6.1. Basolateral amygdala

For proteins measured from the BLA, the weighted correlation matrix is shown in Fig. 6A–and a PCA reduced the dimensionality of the data from 62 to 5 based on the Scree method in n = 28 rats, and as such, 5 components were extracted (Table 3). For consistency, PrL and NAc analyses were also restricted to 5 components. The eigenvalues pertaining to components 1–5 were 12.486, 7.789, 5.601, 4.709, and 4.421, respectively. Components 1–5 explained 20.139%, 12.563%, 9.034%, 7.595%, and 7.141%, respectively, and the cumulative variance explained was 56.472%. While there were no group differences in components 1, 2, and 3 ($Fs_{(1,24)} = 0.001\text{-}1.772$, $ps = 0.204\text{-}0.978$), TgAD rats had higher measures of proteins making up component 4 relative to WT ($F_{(1,24)} = 6.318$, $p = 0.019$, $\eta^2 = 0.208$, $1\text{-}\beta = 0.674$; see Table 3, and Fig. 6B). Additionally, females had higher measures of proteins making up component 5 relative to males and irrespective of genotype ($F_{(1,24)} = 5.130$, $p = 0.033$, $\eta^2 = 0.176$, $1\text{-}\beta = 0.585$). Clusters

(caption on next column)
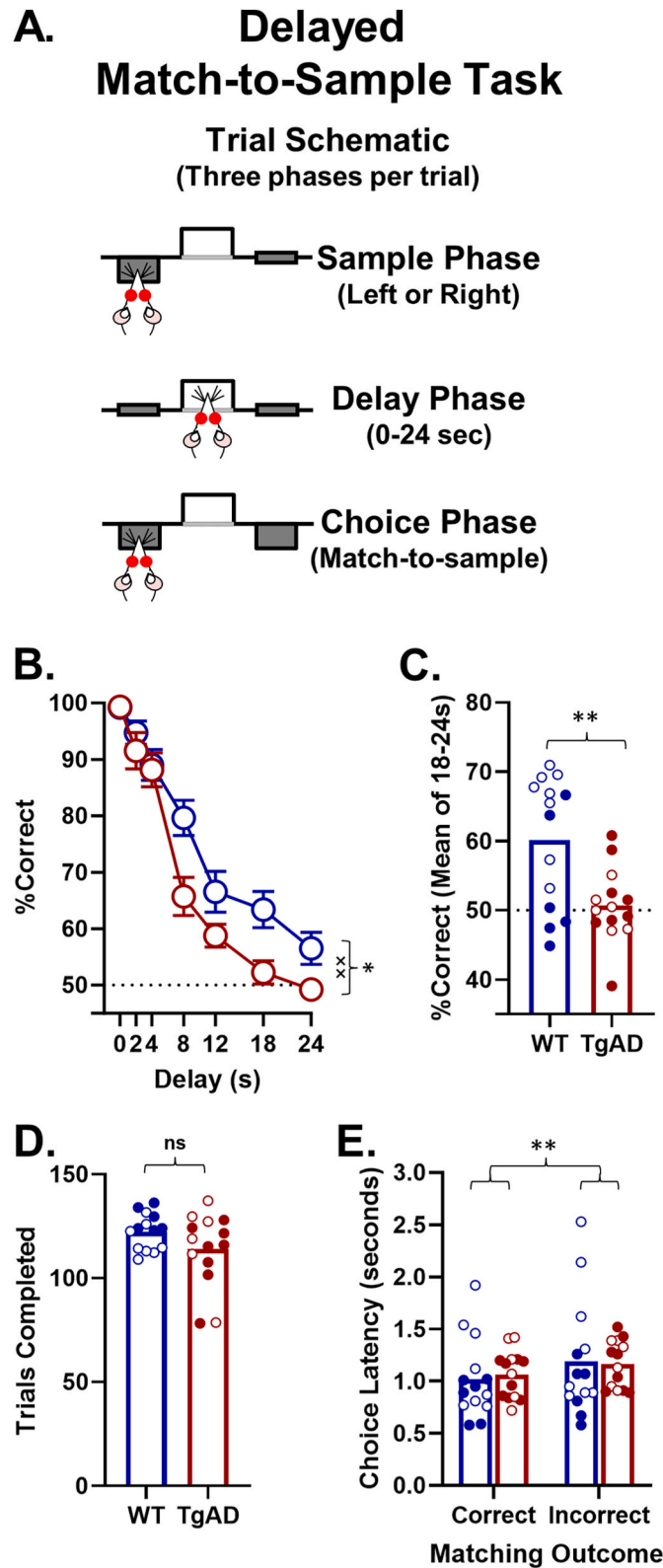
Fig. 4. Delayed match-to-sample task of working memory. A. Task schematic showing phases of each trial. **B.** Working memory was impaired in TgAD rats at longer delays. B. The individual variability of WT and TgAD rats when performance was averaged between 18 and 24 s. TgAD rats had an impaired performance at the longest delays. **D.** Group differences in task performance were not due to differences in ability to engage in the task. **E.** While all rats were slower to respond on incorrect trials, there were no group differences. In all panels, *p < 0.05, **p < 0.01, ××p < 0.01 for the interaction, and ns = not significant; blue represents WT rats, and red represents TgAD rats. Animal numbers in this experiment were n = 14 WT (n = 8 females, n = 6 males) and n = 14 TgAD (n = 6 females, n = 8 males). Females are represented by open circles and males are represented by closed circles. (For interpretation of the references to color in this figure legend, the reader is referred to the Web version of this article.)
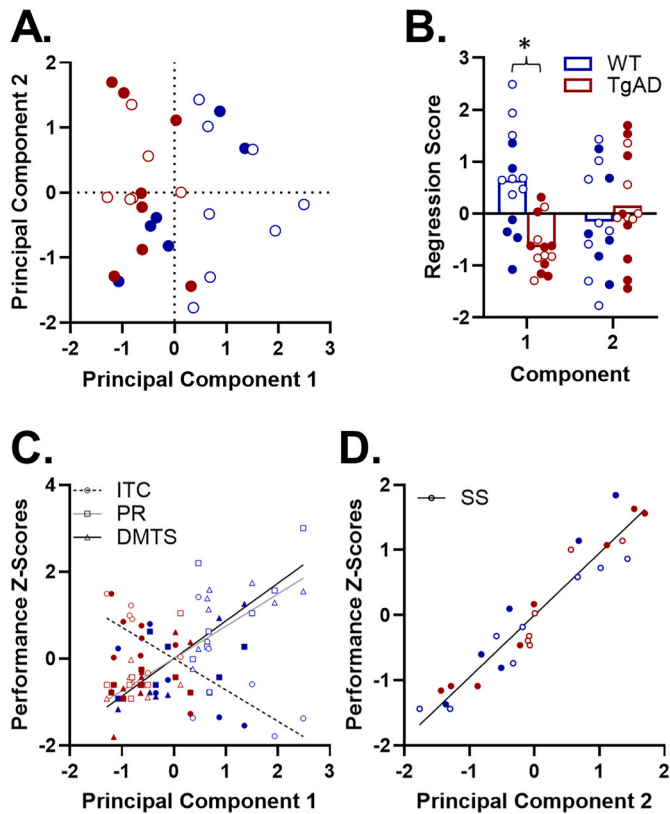
Fig. 5. Principal component analysis on behavioral performances. A. Regression scores show TgAD and WT rat clusters segregated along component 1 which explained variability in intertemporal choice, progressive ratio, and delayed match-to-sample tasks. Component 2 explained the variability in the set-shifting task but did not segregate TgAD rats from WT. **B.** Regression scores for component 1 were significantly different between TgAD and WT rats suggesting clusters were significantly segregated based on task performance for intertemporal choice, progressive ratio, and delayed match-to-sample tasks. **C.** Rats with greater choice of large, delayed rewards were also the same rats that had blunted motivation to obtain food rewards and worse working memory. Importantly, this effect was driven by the TgAD rats. **D.** Performance in set-shift task relative to principal component 2. In all panels, *p < 0.05; blue represents WT rats, and red represents TgAD rats. Animal numbers in this experiment were n = 14 WT (n = 8 females, n = 6 males) and n = 14 TgAD (n = 6 females, n = 8 males). Females are represented by open circles and males are represented by closed circles. (For interpretation of the references to color in this figure legend, the reader is referred to the Web version of this article.)

were explained by gene ontology terms as determined by CytoScape. Specifically, cluster 4 significantly enriched pathways linked to astrocyte activation, microglia activation, and neuroinflammation (Fig. 6C–Supplementary Table S4). As the BLA is necessary for decision making and motivation, we then asked if the variability in component 4 regression scores predicted intertemporal choice or progressive ratio task performances. A linear regression revealed protein cluster (4 nor 5) expression did not predict performance ($Fs_{(1,26)} = 0.040$–0.472, ps = 0.498–0.843, rs = 0.039–0.134; Fig. 6D). The protein-protein interaction networks generated from each cluster are shown in Fig. 6E, and the proteins making up cluster 4 were all increased (Fig. 6B) in TgAD rats, including HGF, IL2, MCP1, IFNg, CD86, TIMP1, RAGE, IL10, IL1β, and TNFα (Fig. 6E), consistent with an increased neuroinflammatory response.

While there were no group differences or interactions between genotype and sex in pTau-Tyr18, pTau-Thr231, and Iba1 ($Fs_{(1,24)} = 0.026$–2.670, ps = 0.115–0.874), there was greater amyloid peptide ($F_{(1,24)} = 30.073$, p < 0.001, $\eta^2 = 0.556$, 1-β = 1.000; Fig. 7Ai) and plaques ($F_{(1,24)} = 14.685$, p < 0.001, $\eta^2 = 0.380$, 1-β = 0.957), pTau-

Ser202-Thr205 ($F_{(1,24)} = 4.273$, p = 0.0497, $\eta^2 = 0.151$, 1-β = 0.510), and GFAP ($F_{(1,24)} = 9.283$, p = 0.006, $\eta^2 = 0.279$, 1-β = 0.832) protein expression in TgAD rats relative to WT. Though there was a trending effect of sex for the amyloid peptide ($F_{(1,24)} = 3.709$, p = 0.066, $\eta^2 = 0.134$, 1-β = 0.456), there were no other effects of sex or interactions ($Fs_{(1,24)} = 0.002$–1.931, ps = 0.177–0.969). An analysis of total protein loaded did reveal a trending interaction between genotype and sex for pTau-Tyr18 ($F_{(1,24)} = 2.958$, p = 0.098, $\eta^2 = 0.110$, 1-β = 0.379). However, follow up pairwise comparisons on simple main effects confirmed no differences between male WT and TgAD ($F_{(1,24)} = 2.047$, p = 0.165) rats and no differences between female WT and TgAD rats ($F_{(1,24)} = 1.004$, p = 0.326). Importantly, our total protein analyses confirmed no differences in total protein between WT and TgAD rats, nor between males and females, nor any other interactions ($Fs_{(24)} = 0.000$–2.052, ps = 0.165–0.995; Supplementary Fig. 2A; See Supplementary Fig. 3A for electropherograms).

A PCA extracted two components (eigenvalue 1: 2.960, 42.289% variance; eigenvalue 2: 1.686, 24.082% variance; 66.371% total variance; Fig. 7Aii). Component 1 best explained Amyloid pathology (0.939 and 0.393, plaques and peptide, respectively), pTau-Ser202-Thr205 (0.627), and GFAP (0.922), whereas component 2 best explained pTau-Tyr18 (0.829), pTau-Thr231 (0.747), and Iba1 (−0.833). While there was a significant effect of genotype for component 1 ($F_{(1,24)} = 16.665$, p < 0.001, $\eta^2 = 0.410$, 1-β = 0.975; Fig. 7Aiii) irrespective of sex ($Fs_{(1,24)} = 0.310$–0.746, ps = 0.298–0.396), there was no effect in component 2 regression scores ($Fs_{(1,24)} = 0.007$–1.377, ps = 0.252–0.936). Fig. 7Aiv shows that the rats with greater amyloid burden, are also the same rats with greater AT8 and GFAP protein, and this effect was driven by TgAD rats.

We then asked if the pathology explained by component 1 would predict intertemporal choice and progressive ratio performance. The pathology explained by component 1 significantly predicted intertemporal choice performance ($F_{(1,27)} = 4.865$, p = 0.036; Fig. 7Av) such that for every unit increase in pathology, there is a 9.57 unit increase in choice of the large, delayed reward ($t_{(27)} = 2.206$, p = 0.036, r = 0.397, B = 9.566). That is, greater BLA pathology predicted greater choice of large, delayed rewards. However, the pathology explained by component 1 did not predict progressive ratio performance ($F_{(1,27)} = 0.800$, p = 0.379). Finally, we determined whether BLA pathology predicted BLA inflammation (cluster 4). Indeed, pathology protein scores from component 1 predicted inflammation protein scores from cluster 4 ($F_{(1,27)} = 18.314$, p < 0.001; Fig. 7Avi). Specifically, for every unit increase in BLA pathology, there was a 0.64 increase in BLA inflammation ($t_{(27)} = 4.279$, p < 0.001, r = 0.643, B = 0.643).

3.6.2. Prelimbic cortex

For proteins measured from the PrL, a PCA reduced the dimensionality of the data from 62 to 5 based on the Scree method in n = 28 rats, and as such, 5 components were extracted. The weighted correlation matrix is shown in Supplementary Fig. 4A. The eigenvalues pertaining to components 1–5 were 16.658, 6.611, 5.086, 4.182, and 3.409, respectively. Components 1–5 explained 26.868%, 10.663%, 8.203%, 6.745%, and 5.499%, respectively, and the cumulative variance explained was 57.979%. The cut-off used for meaningful component loadings was 0.4 (greater than or equal to 0.4) for all loadings in each brain region (Table 3). Each component, therefore, represented proteins that clustered together, and each rats' component regression score represented the degree to which those proteins as a cluster were expressed (higher scores meant greater protein cluster expression). There were no significant differences in cluster expression between WT and TgAD rats within each component ($Fs_{(1,24)} = 0.002$–1.550, ps = 0.225–0.965; Supplementary Fig. 4B). That is, TgAD rats did not show greater or lesser expression of clustered inflammatory markers within the PrL. GO terms representing each cluster are shown in Supplementary Fig. 4C, and the protein-protein interaction networks generated from each cluster are shown in Supplementary Fig. 4D.
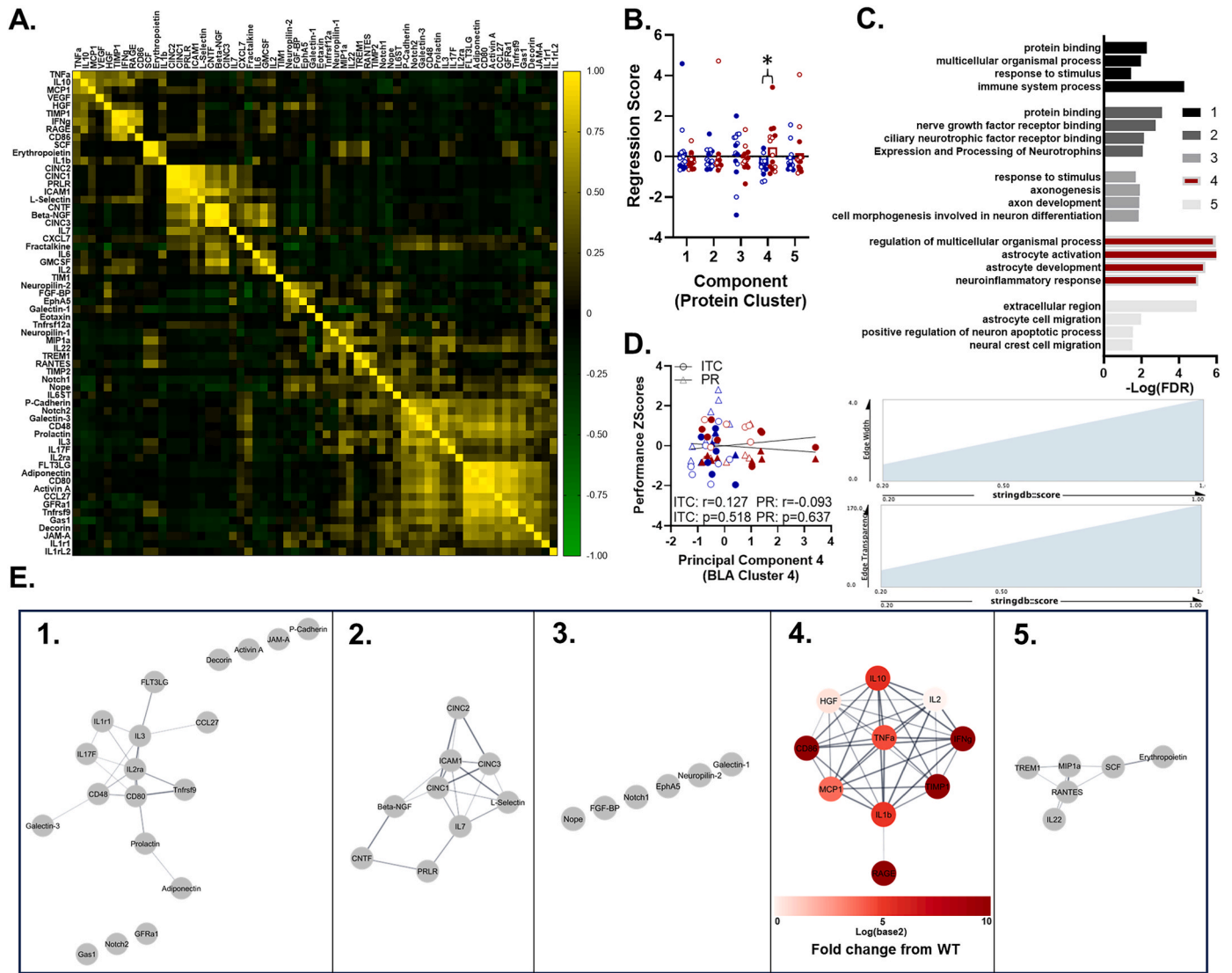
Fig. 6. Inflammatory markers assessed in the BLA. A. Weighted protein correlation network in PrL of WT and TgAD rats as determined by clustergrammer. Color gradient displays r-values. More yellow indicates values closer to r = 1.0 (positive correlations), black indicates r-values near or equal to 0, and more green values indicates values closer to r = −1.0 (negative correlations). **B.** Multivariate ANOVA on PCA regression scores revealed group differences in protein cluster cluster 4. **C.** Cytoscape was used to determine significant (-LogFDR>1.3) gene ontology terms for each cluster. The top terms are displayed. Protein cluster 4 was represented by regulation of multicellular organismal process, astrocyte activation, astrocyte development, and neuroinflammatory response. D. Protein regression scores from cluster 4 did not significantly predict intertemporal choice performance or progressive ration performance. **E.** Protein-protein interaction networks for each cluster as validated by CytoScape. Clusters 1 through 5 are shown independently. Expression of cluster 4 was significantly greater in TgAD rats relative to WT rats indicated by red color. The darker the red, larger the fold-change in each individual protein. In panels B and D, *p < 0.05; blue represents WT rats, and red represents TgAD rats. Animal numbers in this experiment were n=14 WT (n = 8 females, n = 6 males) and n = 14 TgAD (n = 6 females, n = 8 males). Females are represented by open circles and males are represented by closed circles. (For interpretation of the references to color in this figure legend, the reader is referred to the Web version of this article.)

While there were no group differences in the peptide (approx. 7 kDa) detected by our amyloid antibody, any pTau phosphor-sites, and Iba1 ($Fs_{(1,24)}$ = 0.068–3.406, ps = 0.077–0.796; trending amyloid peptide TgAD > WT), we did see significantly more amyloid protein at higher molecular weights (approx. 130 kDa; $F_{(1,24)}$ = 114.654, p < 0.001, η^2 = 0.827, 1-β = 1.000; Fig. 7Bi) and GFAP ($F_{(1,24)}$ = 4.986, p = 0.035, η^2 = 0.172, 1-β = 0.573) signal in the TgAD rats relative to WT. These effects were irrespective of sex ($Fs_{(1,24)}$ = 0.008–1.616, ps = 0.216–0.929) and any interaction between genotype and sex ($Fs_{(1,24)}$ = 0.001–2.886, ps = 0.102–0.976). As there were no effects of sex, sex was excluded in analyses of total protein. An analysis of total protein loaded confirmed no differences in total protein between WT and TgAD rats ($ts_{(26)}$ = 0.392–1.482, ps = 0.150–0.699; Supplementary Fig. 2B; See Supplementary Fig. 3B for electropherograms).

To determine protein-protein associations as done above, we ran a PCA including each protein measure. Two components were extracted (eigenvalue 1: 2.618, 37.399% variance; eigenvalue 2: 1.474, 21.054% variance; 58,452% total variance; Fig. 7Bii). Component 1 best explained pTau-Tyr18 (0.740), pTau-Thr231 (0.819), GFAP (0.442), and Iba1 (0.851), whereas component 2 best explained Amyloid pathology (0.811 and 0.749, plaques and peptide, respectively) and pTau-Ser202-Thr205 (0.643). While there were no group differences in component 1 regression scores ($Fs_{(1,24)}$ = 0.283–0.889, ps = 0.355–0.599), there was a significant effect of genotype for component 2 ($F_{(1,24)}$ = 21.244, p < 0.001, η^2 = 0.470, 1-β = 0.993; Fig. 7Biii) irrespective of sex ($Fs_{(1,24)}$ = 0.256–1.132, ps = 0.298–0.618). Notably, rats with greater amyloid pathology, were also the same rats with greater AT8 protein expression, and this was driven by TgAD rats (Fig. 7Biv).

Table 3

Principal Component Analysis: The Scree method was used to reduce the dimensionality of the data to 5 components. Protein loading scores for each of the 5 components extracted per data set (region) are shown below.

PrL Rotated Component Matrix						BLA Rotated Component Matrix						NAc Rotated Component Matrix					
Tnfrsf9				0.702		Tnfrsf9	0.77					Tnfrsf9	0.495	0.584			0.443
Activin A			0.636			Activin A	0.96					Activin A		0.97			
Adiponectin				0.545		Adiponectin	0.895					Adiponectin		0.688			
CD86	0.833					CD80	0.9					CD80	0.91				
Beta-NGF	0.823					CD86				0.483		CD86					
CD48				0.594		Beta-NGF			0.702	−0.558		Beta-NGF					0.632
CINC1	0.907					CD48	0.879					CD48		0.948			
CINC2	0.412	0.452				CINC1		0.924				CINC1					0.607
CINC3	0.862					CINC2		0.924				CINC2					0.653
CNTF	0.805					CINC3		0.516		−0.539		CINC3				0.446	0.672
CCL27				−0.6		CNTF		0.65		−0.577		CNTF			−0.433		0.627
Decorin			0.751			CCL27	0.774					CCL27	0.787				
Eotaxin						Decorin	0.579					Decorin		0.514			
EphA5						Eotaxin						Eotaxin		0.708			
FGF-BP				0.566		EphA5				0.563		FGF-BP		0.734	0.433		
FLT3LG	−0.402			0.566		Erythropoietin					0.791	FLT3LG		0.704			
Fractalkine				0.683		FGF-BP				0.725		Fractalkine				0.615	
Galectin-1		0.465			0.584	FLT3LG	0.915					Galectin-1				0.854	
Galectin-3				0.411		Fractalkine				−0.601		Galectin-3	0.766				
Gas1		0.615			0.472	Galectin-1				0.534	−0.576	Gas1	0.412	0.626			
GFRa1	−0.491		0.66			Galectin-3	0.776					GFRa1		0.811			
GMCSF	0.589	0.494				Gas1	0.756					GMCSF					0.547
IL6ST						GFRa1	0.884					IL6ST	0.51	0.777			
HGF		0.709				GMCSF				−0.604		HGF	0.43	0.632			
ICAM1		0.564	−0.462		0.426	IL6ST						ICAM1		0.772			
IFNg		0.672				HGF			0.43	0.676		IFNg					
IL1rL2			0.583			ICAM1		0.902				IL1rL2	0.501				
IL1r1						IFNg				0.759		IL1r1	0.474	0.786			
IL10	0.704					IL1rL2						IL10					0.424
IL13	0.826					IL1r1	0.445		0.408			IL13					0.565
IL17F						IL10				0.8		IL17F	0.75				
IL1a	0.597					IL17F	0.424					IL1a			−0.55		
IL1b	0.593					IL1b				0.503	0.464	IL2ra	0.837	0.434			
IL2	0.928					IL2				0.439		IL22	0.924				
IL2ra			0.651			IL2ra	0.508					IL3	0.891				
IL3			0.66	0.469		IL22					0.456	IL6					
IL4	0.832					IL3	0.586				0.472	IL7		0.803			
IL6		0.858				IL6				−0.43		JAM-A		0.489	0.476	−0.413	
JAM-A	−0.404			0.531		IL7			0.683			CXCL5					0.534
CXCL5	0.839					JAM-A	0.594			0.494		L-Selectin					0.7
L-Selectin	0.912					L-Selectin		0.82				MIP1a	0.531				
MCP1	0.782					MCP1					0.49	Neuropilin-1		0.466	0.708		
MIP1a			0.465	0.543		MIP1a					0.872	Neuropilin-2		0.897			
Neuropilin-1					0.601	Neuropilin-1						Nope			0.897		
Neuropilin-2				0.681		Neuropilin-2				0.675		Notch1	0.414		0.765		
Nope		0.606			0.476	Nope				0.731		Notch2	0.66				
Notch1					0.81	Notch1				0.428		P-Cadherin	0.922				
Notch2					0.808	Notch2	0.664					PDGFA					
P-Cadherin			0.604			P-Cadherin	0.667				0.463	Prolactin	0.858				

Table 3 (*continued*)

PrL Rotated Component Matrix

Protein	Loadings
PDGFA	0.654
Prolactin	
PRLR	0.54, 0.535
RAGE	0.766
RANTES	0.499
SCF	
CXCL7	−0.612
TIMP1	0.737
TIMP2	0.456
TNFa	
TREM1	0.439
Tnfrsf12a	0.578
VEGF	0.575

BLA Rotated Component Matrix

Protein	Loadings
Prolactin	0.686
PRLR	0.946
RAGE	0.477
RANTES	
SCF	0.712
CXCL7	0.788
TIM1	0.659
TIMP1	
TIMP2	0.726, 0.456
TNFa	0.752
TREM1	0.439
Tnfrsf12a	
VEGF	0.629

NAc Rotated Component Matrix

Protein	Loadings
PRLR	0.612, −0.527
RAGE	−0.506, 0.423
RANTES	0.442, 0.603
SCF	0.777, 0.601
CXCL7	−0.439
TIMP1	0.856
TIMP2	0.554
TNFa	0.632
TREM1	0.617
Tnfrsf12a	
VEGF	−0.405

We then asked if the pathology explained by component 2 would predict intertemporal choice and working memory performance. The pathology explained by component 2 significantly predicted intertemporal choice performance ($F_{(1,27)} = 6.639$, p = 0.016; Fig. 7Bv) such that for every unit increase in pathology, there is a 10.87 unit increase in choice of the large, delayed reward ($t_{(27)} = 2.577$, p = 0.016, r = 0.451, B = 10.866). That is, greater pathology predicts greater choice of large, delayed rewards. Additionally, the pathology explained by component 2 trended towards significantly predicting working memory performance ($F_{(1,27)} = 2.948$, p = 0.098; Fig. 7Bv) such that for every unit increase in pathology, there is a 2.87 decrease in working memory performance ($t_{(27)} = -1.717$, p = 0.098, r = −0.319, B = −2.865).

3.6.3. Nucleus accumbens

For proteins measured from the NAc, the weighted correlation matrix is shown in Supplementary Figs. 5A and a PCA reduced the dimensionality of the data from 60 to 5 based on the Scree method in n = 28 rats, and as such, 5 components were extracted. The eigenvalues pertaining to components 1–5 were 16.533, 6.865, 6.095, 4.828, and 3.248, respectively. Components 1–5 explained 27.555%, 11.442%, 10.158%, 8.046%, and 5.414%, respectively, and the cumulative variance explained was 62.615% (Table 3). While there were no group differences in components 1, 2, 3, and 4 ($Fs_{(1,24)} = 0.001$–2.263, ps = 0.146–0.970; Supplementary Fig. 5B), female rats had lower measures of proteins making up component 5 relative to males ($F_{(1,24)} = 5.017$, p = 0.035, $\eta^2 = 0.173$, 1-β = 0.575). As there were no genotypic differences in NAc inflammation, no linear regression was tested between cluster scores and behavior. GO terms representing each cluster are shown in Supplementary Fig. 5C, and the protein-protein interaction networks generated from each cluster are shown in Supplementary Fig. 5D.

Together, these data suggest inflammation is occurring in the BLA at a young age in TgAD rats. This effect seems to be specific to the BLA as we did not observe any genotypic differences in the PrL or NAc. Moreover, inflammation in the BLA is not necessarily predicting behavioral performance at this stage of life.

While there were no group differences or interactions between genotype and sex in amyloid peptide, pTau-Tyr18, pTau-Thr231, GFAP, and Iba1 ($Fs_{(1,24)} = 0.003$–1.405, ps = 0.248–0.960), there was greater high molecular weight amyloid protein expression in TgAD rats relative to WT ($F_{(1,24)} = 5.551$, p = 0.027, $\eta^2 = 0.188$, 1-β = 0.618; Fig. 7Ci) irrespective of sex ($Fs_{(1,24)} = 0.636$–0.849, ps = 0.366–0.433) and a trend towards greater pTau-Ser202-Thr205 in females relative to males ($F_{(1,24)} = 4.097$, p = 0.054, $\eta^2 = 0.146$, 1-β = 0.493) irrespective of genotype ($Fs_{(1,24)} = 0.332$–2.080, ps = 0.162–0.570). Notably, amyloid protein was not expressed in most rats in this brain structure suggesting the NAc may be more delayed in amyloid pathology emergence relative to PrL and BLA. An analysis of total protein loaded did reveal a trending effect of sex for Iba1 ($F_{(1,24)} = 4.245$, p = 0.050, $\eta^2 = 0.150$, 1-β = 0.507). However, this did not account for any genotypic differences as our total protein analyses confirmed no differences in total protein between WT and TgAD rats, nor any other effects of sex, nor any other interactions ($Fs_{(24)} = 0.020$–1.922, ps = 0.178–0.889; Supplementary Fig. 2C; See Supplementary Fig. 3C for electropherograms).

As there was a difference in amyloid plaque expression, we used a PCA to ask if there were any pathology protein associations in the NAc. Two components were extracted (eigenvalue 1: 2.032, 29.034% variance; eigenvalue 2: 1.607, 22.954% variance; 51.987% total variance; Fig. 7Cii). Component 1 best explained Amyloid peptide (0.678), pTau-Ser202-Thr205 (−0.367), GFAP (0.695), and Iba1 (0.863), whereas component 2 best explained high molecular weight amyloid protein (−0.620), pTau-Tyr18 (0.638), and pTau-Thr231 (0.818). While there was a trending effect of sex for component 1 ($F_{(1,24)} = 3.792$, p = 0.063, $\eta^2 = 0.136$, 1-β = 0.464), there were no other effects ($Fs_{(1,24)} = 0.823$–0.992, ps = 0.329–0.373; Fig. 7Ciii). There were also no effects in component 2 regression scores ($Fs_{(1,24)} = 0.002$–0.213, ps =

Basolateral Amygdala

Prelimbic Cortex

Nucleus Accumbens
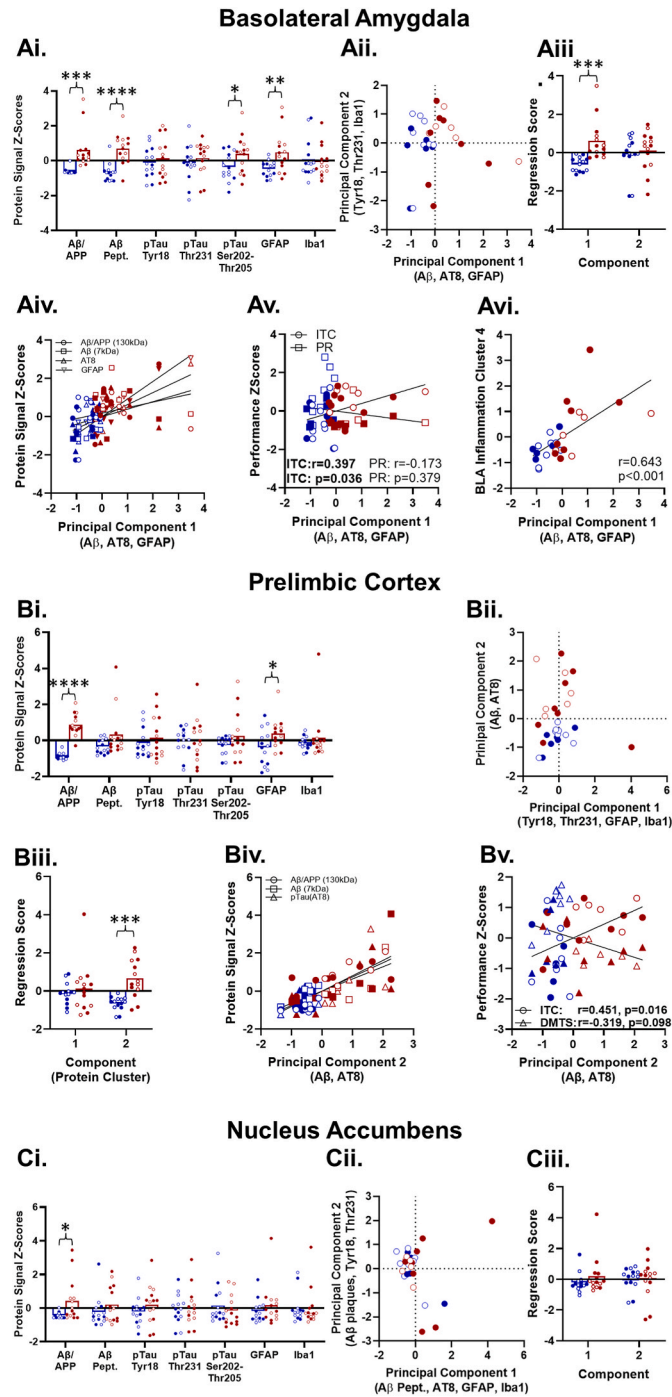
(caption on next page)

Fig. 7. Protein measurements of amyloid, different AD-relevant phosphorylation sites of tau, GFAP, and Iba1 using Biotechne's SimpleWestern system (JESS). Ai-Avi: Basolateral Amygdala. In the BLA, TgAD rats had positive amyloid beta signal at a young adult age. In addition, AT8 and GFAP were significantly greater in TgAD rats. Protein data was transformed to Z-scores for presentation. **Aii.** Principal component analysis. Component 1 explained the variability in amyloid protein, AT8, and GFAP, whereas principal component 2 explained the variability in Tyr18, Thr231, and Iba1. TgAD and WT clusters segregated along principal component 1, but not 2. **Aiii.** Regression scores for component 1 were significantly different between TgAD and WT rats suggesting clusters were significantly segregated based on amyloid, AT8, and GFAP measures, whereas there was no difference in component 2. **Aiv.** Rats with greater amyloid protein burden were also the same rats that had greater AT8 and GFAP protein. Importantly, this effect was driven by the TgAD rats. **Av.** Linear regression between pathology protein component 1 regression scores (x-axis) and behavioral performance Z-scores (y-axis). Pathology protein scores significantly predicted intertemporal choice performance such that rats with greater pathology predicted greater choice of large, delayed rewards. Importantly, this effect was driven by TgAD rats. Protein scores did not predict progressive ratio performance. **Avi.** Linear regression between protein component 1 regression scores (x-axis) and inflammation protein cluster scores (y-axis). Pathology protein scores significantly predicted inflammation protein cluster scores such that rats with greater BLA pathology also had greater BLA inflammation. Importantly, this effect was driven by TgAD rats. **Bi-Bv: Prelimbic cortex. Bi.** In the PrL, TgAD rats had positive amyloid beta signal at a young adult age. In addition, GFAP was significantly greater in TgAD rats. Protein data was transformed to Z-scores for presentation. **Bii.** Principal component analysis. Component 1 explained the variability in Tyr18, Thr231, GFAP, and Iba1, whereas principal component 2 explained the variability in amyloid protein and AT8. TgAD and WT clusters segregated along principal component 2, but not 1. **Biii.** Regression scores for component 2 were significantly different between TgAD and WT rats suggesting clusters were significantly segregated based on amyloid and AT8 measures, whereas there was no difference in component 1. **Biv.** Rats with greater amyloid protein burden were also the same rats that had greater AT8 protein. Importantly, this effect was driven by the TgAD rats. **Bv.** Linear regression between protein component 2 regression scores (x-axis) and behavioral performance Z-scores (y-axis). Protein scores significantly predicted intertemporal choice performance such that rats with greater pathology predicted greater choice of large, delayed rewards. Importantly, this effect was driven by TgAD rats. In addition, protein scores tended to predict working memory performance such that rats with greater pathology predicted worse working memory performance. This effect was also driven by TgAD rats. **Ci-Ciii: Nucleus accumbens. Ci.** In the NAc, TgAD rats had positive amyloid beta signal at a young adult age. However, there was individual variability in TgAD rat NAc amyloid protein such that not all TgAD rats showed amyloid burder in young adulthood. Moreover, no other proteins were significantly different. Protein data was transformed to Z-scores for presentation. **Cii.** Principal component analysis. Component 1 explained the variability in amyloid peptide protein, AT8, GFAP, and Iba1, whereas principal component 2 explained the variability in amyloid plaques, Tyr18, and Thr231. TgAD and WT clusters did not segregate along any component. **Ciii.** There were no group differences in regression scores for any component. In all panels, *p < 0.05, ***p < 0.001; blue represents WT rats, and red represents TgAD rats. Animal numbers in this experiment were n = 14 WT (n = 8 females, n = 6 males) and n = 14 TgAD (n = 6 females, n = 8 males). Females are represented by open circles and males are represented by closed circles. (For interpretation of the references to color in this figure legend, the reader is referred to the Web version of this article.)
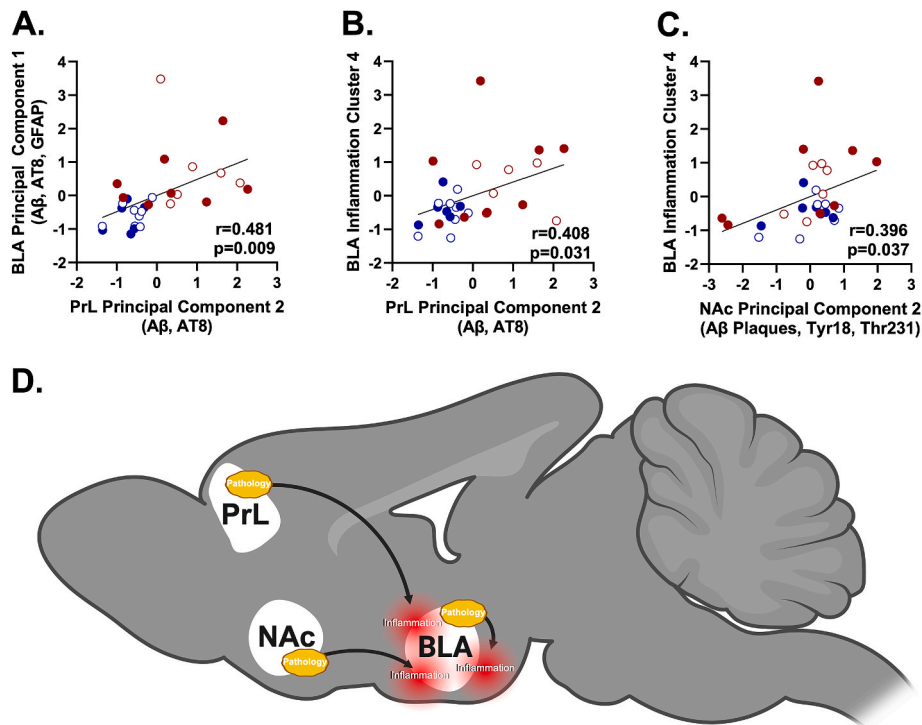
Fig. 8. Linear regression scores between measured pathology and inflammation scores from each brain structures: a pathology circuit analysis. A. AD-like pathology in the PrL predicted AD-like pathology in the BLA such that for every unit increase in PrL pathology there is an increase in BLA pathology (i.e., rats with grater PrL pathology also had greater BLA pathology). **B.** AD-like pathology in the PrL predicted BLA inflammation such that rats with grater PrL pathology also had greater BLA inflammation. **C.** Though no significant differences in regression scores were measured in NAc, amyloid pathology was greater in TgAD rats. As such, we tested whether the component explaining amyloid plaques in the NAc of TgAD rats also predicted BLA inflammation. Indeed, AD-like pathology in the NAc predicted BLA inflammation. **D.** Model of intra-region pathology interactive with BLA inflammation. Interestingly, pathology in each brain structure within this circuit predicted BLA inflammation. In all panels, blue represents WT rats, and red represents TgAD rats. Animal numbers in this experiment were n = 14 WT (n = 8 females, n = 6 males) and n = 14 TgAD (n = 6 females, n = 8 males). Females are represented by open circles and males are represented by closed circles. (For interpretation of the references to color in this figure legend, the reader is referred to the Web version of this article.)

0.002–0.649; Fig. 7Ciii). As there were no differences, no other follow-up analyses were conducted.

3.7. Associations between pathology, inflammation, and behavioral performance

The PrL, BLA, and NAc are interconnected and support cognitive and emotional domains critical to the decision-making process. As such, it is likely this interconnectivity can result in pathogenic influences between regions. To test if pathology in one brain structure predicted pathology in another, we used a linear regression on PCA regression scores.

We tested the pathology scores explained by PrL component 2, BLA component 1, and NAc component 2, all of which strongly loaded amyloid protein expression. Indeed, the pathology explained by PrL component 2 predicted the pathology explained by BLA component 1 ($F_{(1,27)}$ = 7.832, p = 0.010; Fig. 8A) such that for every unit increase in PrL pathology, there was a 0.48 unit increase in BLA pathology ($t_{(27)}$ = 2.799, p = 0.010, r = 0.481, B = 0.481). In contrast, pathology between PrL and NAc or NAc and BLA was not predictive ($Fs_{(1,24)}$ = 01.319–1.632, ps = 0.213–0.249; Supplementary Figs. 6A–B).

As the BLA appeared to be a hub for early brain inflammation, we then asked if pathology in each structure would predict the genotypic differences in BLA protein cluster 4 expression. Indeed, expression of the inflammatory proteins making up BLA cluster 4 was predicted by the pathology explained by PrL component 2 ($F_{(1,27)}$ = 5.206, p = 0.031; Fig. 8B), BLA component 1 (as shown above in Fig. 8B), and NAc component 2 ($F_{(1,27)}$ = 4.824, p = 0.037; Fig. 8C). Specifically, for every unit increase in PrL pathology, there is a 0.41 increase in BLA inflammation ($t_{(27)}$ = 2.282, p = 0.031, r = 0.408, B = 0.408); for every unit increase in BLA pathology, there is a 0.64 increase in BLA inflammation (as shown above in Fig. 7Avi); and for every unit increase in NAc pathology, there is a 0.40 increase in BLA inflammation ($t_{(27)}$ = 2.196, p = 0.037, r = 0.396, B = 0.396). These results suggest pathology in this integrated circuit influences inflammation in the BLA of young adult TgAD rats. Additionally, brain inflammation and aberrant brain activity are related, and as such, the early inflammation observed in the current study is consistent with the hyperexcitability in the BLA of young adult TgAD rats we previously reported (Hernandez et al., 2022a).

4. Discussion

Characterizing early behavioral perturbations is critical in detecting risk factors and their interactions for individuals on a trajectory to develop AD. In this study, we measured early deficits in several cognitive and emotional domains. Specifically, we found intertemporal choices were maladaptive in young adult TgAD rats, as revealed by their greater choice of large rewards not translating into greater reward yields. Importantly, this behavioral alteration in TgAD rats was not due to learning impairments, procedural deficits, hunger state, delay perception, or differences in the weightings of reward magnitude ratios. We also measured decreased motivation to obtain food rewards which would suggest enhanced apathy in young adult TgAD rats, and this effect was not due to differences in general motor activity. While there was preserved cognitive flexibility in young adult TgAD rats, TgAD rats did exhibit impaired working memory. The decision-making process depends on intact working memory and motivation (Gunn and Finn, 2013; Hernandez et al., 2017; Huckans et al., 2011; Shamosh et al., 2008). In our study, we show that rats with worse working memory and motivation deficiencies more frequently chose the large, delayed reward.

Decision making is critically dependent upon a broad network including the mPFC, BLA, and NAc. Additionally, the PrL of the mPFC sufficiently supports working memory performance and delay-based decision making (Bailey et al., 2016; Dietrich and Allen, 1998; Floresco et al., 2008b; Fobbs and Mizumori, 2017; Hernandez et al., 2022b; Orsini et al., 2015; Peters and Büchel, 2011). Our study also sought to determine if inflammation and pathology in a network supporting these

cognitive and emotional domains explained behavioral deficiencies at an individual level. While increased inflammation was specific to the BLA of TgAD rats, we did measure increases to amyloid pathology in all regions assessed. Moreover, we measured greater GFAP protein in the PrL and BLA with an additional measure of greater phospho-tau specific to the BLA of young adult TgAD rats. While inflammation in the BLA did not predict behavioral performance, we found AD-related pathology in the PrL and BLA did predict intertemporal choices (PrL and BLA pathology) and working memory (PrL pathology). Finally, we determined that AD-related pathology in the PrL, BLA, and NAc was predictive of inflammation in the BLA.

There have been few studies addressing intertemporal choice in rodent mouse models of AD and none in rat models of AD. While the current literature on intertemporal choice in mouse models of AD is mixed with one study using surgical induction of amyloid pathology in mice reporting increased discounting of large, delayed rewards (Arun-Sundar et al., 2018), our results are consistent with at least two other studies showing greater choice of delayed rewards when given the option between water and a delayed 0.5% saccharin solution in an APP mutant mouse model (Masuda et al., 2016; Sutoko et al., 2021). In humans, the literature is also mixed. Some studies show AD is associated with greater discounting of large, delayed rewards (El Haj et al., 2020, 2022; Geng et al., 2020; Manuel et al., 2020; Thoma et al., 2017), and one of these studies found that only when primed with a negative emotional state do AD patients become more impulsive (Manuel et al., 2020), though other studies show no differences (Beagle et al., 2020; Bertoux et al., 2015; Coelho et al., 2017).

To incentivize our rats to engage in the task, it was necessary to restrict their food intake. Rats were placed on a food restricted schedule that dropped their weight to 85% of their *ad libitum* food intake. As such, it was possible the genotypic differences in decision making were influenced by hunger state. Indeed, our recent publication showed differences in baseline weights such that TgAD rats consistently weighed more than WT rats across the lifespan (Hernandez et al., 2022a), and thus there may be potential differences in metabolism between groups. Moreover, three recent studies in this rat model did find transcriptomic changes to genes associated with metabolism in young adults (Anderson et al., 2023), gut microbiome dysbiosis at middles ages (Nagarajan et al., 2023), and impaired glucose and insulin metabolic homeostasis in young adults (Srivastava et al., 2023). However, within the context of our own study, the hunger state dependency control experiment showed, despite being satiated (indicated by an equivalent increase in trial omissions in both groups), decision making was unaltered in all rats (indicated by the null effect of the feeding schedule on choices), and as such, the maladaptive decision-making phenotype reported here is not due to hunger-state dependency. Importantly, food-restricting rats to 80% of their *ad libitum* weight does not induce behavioral differences relative to controls (Heiderstadt et al., 2000) but it can improve behavior (Bruce-Keller et al., 1999; Chowdhury et al., 2021; Kenny et al., 2014; Orsini et al., 2004; Parikh et al., 2016; Riul and Almeida, 2020; Stewart et al., 1989) and enhance resistance to excitotoxin-induced degeneration (Bruce-Keller et al., 1999). Therefore, we do not believe the degree of food restriction had an impairing effect on the TgAD rats, and it is possible this modest food restriction protocol could have prevented more severe impairments.

Due to the fixed trial design of our study, greater choice of large, delayed rewards (or a greater ability to delay gratification) could have resulted in a greater number of rewards earned by TgAD relative to WT rats. That is, the cost of the delay can be outweighed by the benefit of earning a greater number of rewards. Although they did have a greater preference for large, delayed rewards, a seemingly beneficial preference, TgAD rats earned less rewards than was predicted. As such, we argue in the case of TgAD rats, choosing the large, delayed reward was an inappropriate (or maladaptive) decision strategy. Consistent with our findings, at least one other study reported a lower reward yield in a hippocampal-dependent spatial memory task (Tournier et al., 2021).

Altering the small to large reward ratio from 4:1 to 3:1 to 2:1 showed TgAD rats maintained their greater preference for the larger, delayed reward without earning significantly more rewards. The identity of the large reward lever remained the same throughout testing, so it is possible the TgAD rats were perseverating on the large reward lever across successive blocks. However, the experiment designed to test delay insensitivity also shows the ability to shift their choice from one lever to the other was preserved in the TgAD rats. As such, differences in choice preference were not explained by perseveration. We, therefore, considered altered emotional affect and executive dysfunction as an explanation of TgAD rats' low reward yield despite greater choice of large, delayed rewards.

Emotional affect strongly influences decision making (Gunn and Finn, 2013; Hernandez et al., 2017; Huckans et al., 2011; Shamosh et al., 2008). Apathy is blunted motivation that is not attributable to impaired cognition or emotional distress (Mann, 1990). Thus, motivational deficits are indicative of apathy (Resnick et al., 1998), which is a well-established phenotype of individuals with AD (Craig et al., 1996; Kuzis et al., 1999; Levy et al., 1998; McPherson et al., 2002). Consistent with this, TgAD rats completed a lower number of lever presses to obtain food rewards relative to WT rats. This was not due to lowered incentive solely due to the magnitude of the small reward, as TgAD rats also did not increase their responding to a larger reward, whereas WT rats did. The fact that young adult TgAD rats performed less lever presses than young adult WT rats under both reward conditions together with the fact that TgAD rats did not increase their responding under a higher magnitude reward condition suggests greater apathy toward normally rewarding reinforcers. This blunted emotional affect could at least in part explain their decision-making outcomes. That is, general reward apathy prevented TgAD rats from maximizing their reward earnings, and the consequence of such apathy was sub-optimal outcomes. An important finding of our study is that the apathy phenotype in TgAD rats was driven mostly by the female TgAD rats. Indeed woman are disproportionately affected by AD (Bachman et al., 1992; Fratiglioni et al., 1997; Gambassi et al., 1999), and apathy could be one early behavioral marker of AD worth exploring in our model.

In addition to emotion guiding our decisions, executive functions are critical to the decision-making process. Using a hippocampus-dependent spatial learning memory task, previous studies have shown increases in the number of trials necessary to learn a location change to an escape well (Cohen et al., 2013), while others have shown increases in the latency to reach a changed escape platform location (Kelberman et al., 2022; Rorabaugh et al., 2017). However, these effects were mostly age dependent. Specifically, while the Cohen et al. (2013) study mentioned there was a trend toward a significant increase in trials for the new well location, they did not report their statistical results in the young adult TgAD rats. Additionally, the Rorabaugh et al. (2017) study showed well-controlled increases in latency to locate the new escape platform location in 16-month-old TgAD rats, but their results in the 6-month-old rats also show slower swim speeds. However, a modest impairment in 6-month-old TgAD rats was found in another study (Kelberman et al., 2022). There are major differences in methodology between our study and these previous studies on cognitive flexibility in TgAD. Indeed, the tasks and brain structure dependence are dissimilar and dissociable (Floresco, 2013; Floresco et al., 2008a), and as such, the dissimilarity would account for differences between study outcomes. While reversal learning may not require the medial prefrontal cortex (Boulougouris et al., 2007; Floresco et al., 2008a), strategy shifting employed in our study does (Floresco et al., 2008a). Moreover, spatial reversal maze-based tasks are heavily dependent on the hippocampus and also require a broader network engagement (Malá et al., 2015) and thus may be more sensitive to network disruptions in AD. Finally, it is possible that the order of strategies presented could explain the null effects. For example, there were fewer trials to learn the lever location rule than the visual discrimination rule. It is possible the attentional set shift from visual discrimination to lever location was too easy, and reversing the

attentional set may be sensitive enough to detect strategy set-shift impairments in these young adults.

While cognitive inflexibility does not explain intertemporal choice differences, the inability to maintain recent trial information about reward and cost (delays) would be detrimental to making future decisions. Indeed, young adult TgAD rats were working memory impaired relative to young adult WT rats. Notably, there was no impairment at short delays. A recent study showed no performance differences in a delayed non-match-to-sample (DNMTS) task at 5 months of age in this rat model of AD (MuñozMoreno et al., 2018). However, it is possible the null effect was due to the difficulty of the DNMTS task vs the DMTS task employed in our current study, as the WT rats were performing, on average, under 80 percent during what the authors considered short delays (MuñozMoreno et al., 2018). Moreover, it was not clear if differences may have been driven by the longest delays, as the data were binned into delays less than or greater than 15 s. Another study did report memory impairments as assessed by a Y-maze task in young adult TgAD rats (Anderson et al., 2023), although others found no impairment in a hippocampal dependent Y-maze task in young adults TgAD rats (Ceyzériat et al., 2024). Here, we chose a task that isolated the functional output of the mPFC (executive function) and is not hippocampal dependent (Sloan et al., 2006). In our study, it is possible poor working memory resulted in less retention of the negative attributes accompanied by a larger reward coupled with a higher cost. Notably, impaired working memory is a known characteristic of early dementia (Baddeley et al., 2017; Morris, 1994; Stopford et al., 2012).

Another important finding of our study is the association between motivation, working memory, and decision-making outcomes. Specifically, rats with lower reward motivation and worse working memory also chose the large, delayed reward more than rats with higher motivation and better working memory performance. Consistent with our findings, a recent study also showed lower motivation is associated with greater choice of large, delayed rewards in non-diseased (or otherwise healthy) aged rats (Hernandez et al., 2017). However, in contrast to our findings, previous studies have linked better working memory with greater choice of large, delayed rewards (Bobova et al., 2009; Hernandez et al., 2017; Shamosh et al., 2008; Shimp et al., 2015). The negative relationship between reward motivation and choice of large, delayed rewards was potentially driven by greater salience toward reward immediacy and not so much reward magnitude, as greater motivation predicted less choice of large rewards. Relatedly, the negative relationship between worse working memory and greater choice of delayed rewards suggests the cost vs benefits of the delayed reward was better remembered in rats with better working memory. Additionally, the relationship between greater motivation and better working memory also suggests motivation may play into boosting the salience of rewards or costs while information is temporarily maintained in working memory. As such, motivational deficiencies and working memory impairments explain the maladaptive decision making observed in young adult TgAD rats. Interestingly, we also showed differences between WT and TgAD were larger in females, consistent with at least one other study (Berkowitz et al., 2018). We also considered whether the order of testing influenced performance. While the literature on testing order effects is mixed with one study showing no effect (HuiYin, 2014) and another showing testing order does have an effect on outcomes (Blokland et al., 2012), the aging literature would suggest that engaging in cognitively demanding tasks that promote plasticity in the aging brain may create cognitive reserve or promote resilience in old age and AD (Fabrigoule et al., 1995; Scarmeas and Stern, 2003; Tucker and Stern, 2011; Verghese et al., 2003; Whalley et al., 2004; Wilson et al., 2002). Therefore, having prior training may benefit testing in later tasks. For example, by the time rats began working memory testing, it is possible prior operant training experience could have either improved task performance or at least buffered more severe impairments. Finally, given the well-established relationship between decision making, executive function, and motivational affect (Bobova et al., 2009; Hernandez et al.,

2017; Shamosh et al., 2008; Shimp et al., 2015), it is reasonable to expect similar outcomes if the order of testing were reversed. Notably, relative to their WT counterparts, young adult TgAD rats did not show any deficits in learning task contingencies during behavioral shaping, which contrasts what has been previously observed in spatial learning tasks (Bernaud et al., 2022; Kelberman et al., 2022; Rorabaugh et al., 2017).

The BLA serves as an integrative hub of emotional valence in this functional circuitry, and we previously reported early BLA synaptic dysfunction in young adult TgAD rats (Hernandez et al., 2022a). As such, we tested whether early-life expression of Alzheimer's pathology and neuroinflammation in the mPFC (PrL), BLA, or NAc explained individual differences in behavioral performance.

Based on our PCA, several markers of inflammation were clustered together (based on components) and increased in the BLA of TgAD relative to WT rats. These markers included HGF, IL2, MCP1, IFNg, CD86, TIMP1, RAGE, IL10, IL1β, and TNFα. Several studies have implicated many of these as markers of peripheral inflammation in Alzheimer's disease patients (Bettcher and Kramer, 2014; Leung et al., 2013; Maes et al., 1999; O'Bryant et al., 2016; Popp et al., 2017). However, the directionality of differential expression is mixed. Consistent with our results, previous studies have also shown increases in MCP1 (Galimberti et al., 2006), HGF (Tsuboi et al., 2003), CD86 (Sabaie et al., 2023), TIMP1 (Yao et al., 2018), RAGE (Yan et al., 1996), and IL1β (Grammas and Ovase, 2001) in AD patients. In addition, IL10 was shown to correlate negatively with ventricular volume in patients with AD, for example, smaller ventricular volumes correlate with greater levels of peripheral IL10 (Leung et al., 2013). In contrast, studies have reported mixed findings regarding TNFα in patients with AD, including reports of no change (Leung et al., 2013), increases (Alvarez et al., 2007; Grammas and Ovase, 2001; Holmes et al., 2009; Tarkowski et al., 1999), and even decreases (Lanzrein et al., 1998) within specific brain regions. However, one study showed the discrepancies between studies may be attributed to differences in the samples used to measure the analyte, for example, plasma vs serum vs cerebral spinal fluid (O'Bryant et al., 2016). Whether peripheral increases in these markers promote pathogenic or protective mechanisms (Tarkowski et al., 1999), or are independent from brain pathology, remains unclear. Indeed, our study sought to measure these markers directly in brain tissue, and further, with regional specificity. There have been positive reports of inflammation in this rat model and two mouse models (the TgAPPsw and PS1/APPsw) at young adult and later ages in other structures, for example, the hippocampus (Bac et al., 2023; Cohen et al., 2013; Patel et al., 2005; Wu et al., 2020). In our current study, and consistent with at least one other study (Ceyzériat et al., 2024), we demonstrate specific markers of inflammation are not expressed uniformly across the brain at young ages, and furthermore, we highlight potentially important markers of inflammation that are strongly related to each other based on protein-protein interactions which could predict AD pathology early in life.

In addition to inflammation in the BLA, there was significant amyloid and tau pathology, as well as an association between inflammation, pathology, and gliosis. Importantly, this AD-like pathology in young adult TgAD rats did explain the individual variability in intertemporal choice performance such that rats with greater pathology also had greater choice of large, delayed rewards. Moreover, AD-like pathology was also predictive of BLA inflammation. Thus, it is possible the neurobiological changes in the BLA driven by pathology and inflammation account for decision making behavior. Indeed, our recent publication demonstrated that the BLA is hyperexcitable even at early ages in TgAD rats and that this hyperexcitability associated with behavioral impairments in fear extinction (Hernandez et al., 2022a). It is well-established that hyperexcitability can drive inflammation, and in turn, greater inflammation can drive hyperexcitability in a vicious cycle (Inagaki et al., 2012; Liu et al., 2016; Patel et al., 2017; Targa Dias Anastacio et al., 2022; Wolinski et al., 2022; Zaitsev et al., 2021). Inactivating the BLA during choice outcomes biased young adult rats

toward greater choice of small, immediate rewards thus suggesting that under normal conditions, greater activity during sub-optimal outcomes would bias choice towards large, delayed rewards (Hernandez et al., 2019). As such, inflammation and pathology in the BLA could be explained by greater activity in the BLA of young adult TgAD rats previously reported (Hernandez et al., 2022a), and furthermore an inflammation-hyperexcitability cycle in BLA may account for the maladaptive choices reported in our young adult TgAD rats.

While there was no increase in markers of inflammation in the PrL of young adult TgAD rats, amyloid pathology was present and associated with tau and GFAP, suggesting early perturbations in glial processes. It is not entirely surprising that inflammation in the PrL is not yet measurable as these TgAD rats are still in young adulthood, and moreover, there is evidence that other perturbations linked to AD, such as synaptic function and neuronal excitability, occur in the absence of overt AD pathology (Mondadori et al., 2006; Stargardt et al., 2015). Though not in young adults, a recent study in middle aged TgAD rats reported increased cytokines in the hippocampus and surrounding cortex at approximately 12 months (Wu et al., 2020). While cytokines and chemokines were not analyzed, a recent study in young adult (6 mo) and middle aged (12 mo) TgAD rats reported an increase in the number of GFAP + cells in all three subfields of the hippocampus that was driven by 12 month old TgAD rats, and additionally, this same study reported an increase in the number of Iba1+ cells of the dentate gyrus at 6 and 12 months of age (Kelberman et al., 2022). Notably, Alzheimer's-like pathology in the PrL was predictive of intertemporal choice and tended to predict working memory performance, and consistently, at least one other study showed greater hippocampal amyloid and tau pathology correlated with worse spatial learning (Bac et al., 2023). The PrL is critical to the internal representation of information no longer in the environment, information that is necessary in decision making and working memory tasks (Churchwell et al., 2009; Floresco and Magyar, 2006; Floresco et al., 2008b; Hernandez et al., 2018; Hernandez et al., 2022b; Sloan et al., 2006; Yang et al., 2014). As such, Alzheimer's pathology may be disrupting the neuronal processes required to maintain the short-lived information about reward costs.

Though there was more Aβ in NAc of TgAD rats relative to WT, similar to other reports (Ceyzériat et al., 2021; Tournier et al., 2021), there was variability in the extent of the amyloid pathology suggestive of a delayed onset in subcortical structures as seen in older individuals at risk for AD (Levin et al., 2021). Given more advanced age, we would expect more consistent measures of amyloid pathology (potentially tau pathology) in TgAD rats.

It should be noted that cognitive testing in our study could have also buffered the degree to which pathology may have been expressed. For example, TgAD rats with more WT-like cognitive scores may have buffered against more severe pathology. Several studies have shown cognitively engaging tasks promote cognitive reserve in aging and AD (Fabrigoule et al., 1995; Scarmeas and Stern, 2003; Tucker and Stern, 2011; Verghese et al., 2003; Whalley et al., 2004; Wilson et al., 2002). However, cognitive reserve and resilience is thought to typically occur despite similar pathology between individuals and groups (Nelson et al., 2021; Reed et al., 2010; Wilson et al., 2002; Xu et al., 2019; Zahodne et al., 2013) such that individuals with high reserve perform better than predicted given their pathology severity. While cognitive reserve can buffer against cognitive decline, it does not necessarily buffer against pathology severity, and variability in pathology severity can be, nonetheless, predictive of variability in cognitive performance (Bac et al., 2023; Jansen et al., 2018; MuñozMoreno et al., 2018; Shokouhi et al., 2019; Vemuri et al., 2015).

At least two studies have demonstrated whole-brain functional network connectivity perturbations as early as young adulthood (Anckaerts et al., 2019; MuñozMoreno et al., 2018). Similarly to these prior studies, our study shows early AD-like pathology and inflammation. In addition, our study adds that early behavioral impairments are associated with AD-like pathology in a circuit relevant to the behavioral

tasks employed, whereas those studies did not find or test for behavioral impairments. The BLA, PrL, and NAc are interconnected, and as such, we propose a hypothesis-driven model showing perturbations driven by pathology within these structures influences the increase in BLA inflammation (Fig. 8D). Consistent with one other study (Ceyzériat et al., 2024), our results suggest brain inflammation in AD is non-uniform and is region-specific in early phases of AD, as expected given the time course of pathology spread in humans. Indeed, the BLA may be one of a few important hubs undergoing changes indicative of early pathology and inflammatory processes occurring in Alzheimer's disease. This idea is consistent with the fact that behaviors critically dependent upon the amygdala, like fear memory encoding and extinction, are some of the first behavioral phenotypes observed in AD patients (Hamann et al., 2002; Hoefer et al., 2008).

4.1. Conclusions

There are several important findings in this study. Whereas others have shown early impairments on hippocampal-dependent learning and memory (Bernaud et al., 2022; Kelberman et al., 2022; Rorabaugh et al., 2017), and we have shown early impairments in BLA-dependent memory (Hernandez et al., 2022a), in our current study, we showed evidence for early changes to higher order cognition and emotional processing in a rat model of AD. Specifically, we showed maladaptive decision making associated with blunted motivation and impaired working memory performance. Another key finding of our work is that emotional/motivational deficits were driven by sex (Female TgAD rats responded less than Female WT rats). We also showed that behavioral performances supported by PrL (intertemporal choice and working memory) and BLA (intertemporal choice) were predicted by AD-like pathology in said brain structures. Additionally, our findings show that pathology in this network associates with inflammation in the BLA, and as such, we highlight the BLA as one of the more vulnerable and inflammation-susceptible regions in prodromal stages of AD as shown in other regions (Cohen et al., 2013; Kelberman et al., 2022; Rorabaugh et al., 2017). Taken together, our results suggest that early and modest neurobiological perturbations within the relevant circuitry penetrate to the level of behavioral observations, indicating impaired behavioral performances early in life may be useful in screening for neurodegenerative disease trajectories and predicting disease severity.

CRediT authorship contribution statement

Caesar M. Hernandez: Conceptualization, Data curation, Formal analysis, Funding acquisition, Investigation, Methodology, Project administration, Resources, Software, Supervision, Validation, Visualization, Writing – original draft, Writing – review & editing. **Macy A. McCuiston:** Data curation, Investigation, Methodology, Visualization, Writing – review & editing. **Kristian Davis:** Data curation, Methodology. **Yolanda Halls:** Data curation, Investigation, Methodology, Validation. **Juan Pablo Carcamo Dal Zotto:** Data curation, Investigation, Methodology, Validation. **Nateka L. Jackson:** Data curation, Investigation, Methodology, Project administration, Resources, Validation. **Lynn E. Dobrunz:** Funding acquisition, Resources, Writing – review & editing. **Peter H. King:** Conceptualization, Methodology, Validation, Writing – original draft. **Lori L. McMahon:** Funding acquisition, Project administration, Resources, Writing – original draft, Writing – review & editing.

Declaration of competing interest

The authors declare that they have no known competing financial interests or personal relationships that could have appeared to influence the work reported in this paper.

Data availability

Data will be made available on request.

Acknowledgements

Appendix A. Supplementary data

Supplementary data to this article can be found online at https://doi.org/10.1016/j.bbih.2024.100798.

References

Abramowski, D., Rabe, S., Upadhaya, A.R., Reichwald, J., Danner, S., Staab, D., Capetillo-Zarate, E., Yamaguchi, H., Saido, T.C., Wiederhold, K.-H., Thal, D.R., Staufenbiel, M., 2012. Transgenic expression of intraneuronal Aβ42 but not Aβ40 leads to cellular Aβ lesions, degeneration, and functional impairment without typical Alzheimer's disease pathology. J. Neurosci. 32, 1273–1283. https://doi.org/10.1523/JNEUROSCI.4586-11.2012.

Albert, M.S., 1996. Cognitive and neurobiologic markers of early Alzheimer disease. Proc. Natl. Acad. Sci. U.S.A. 93, 13547–13551. https://doi.org/10.1073/pnas.93.24.13547.

Alvarez, A., Cacabelos, R., Sanpedro, C., García-Fantini, M., Aleixandre, M., 2007. Serum TNF-alpha levels are increased and correlate negatively with free IGF-I in Alzheimer disease. Neurobiol. Aging 28, 533–536. https://doi.org/10.1016/j.neurobiolaging.2006.02.012.

Alzheimer's Association, 2021. 2021 Alzheimer's disease facts and figures. Alzheimers Dement 17, 327–406. https://doi.org/10.1002/alz.12328.

Anckaerts, C., Blockx, I., Summer, P., Michael, J., Hamaide, J., Kreutzer, C., Boutin, H., Couillard-Després, S., Verhoye, M., Van der Linden, A., 2019. Early functional connectivity deficits and progressive microstructural alterations in the TgF344-AD rat model of Alzheimer's Disease: a longitudinal MRI study. Neurobiol. Dis. 124, 93–107. https://doi.org/10.1016/j.nbd.2018.11.010.

Anderson, T., Sharma, S., Kelberman, M.A., Ware, C., Guo, N., Qin, Z., Weinshenker, D., Parent, M.B., 2023. Obesity during preclinical Alzheimer's disease development exacerbates brain metabolic decline. J. Neurochem. https://doi.org/10.1111/jnc.15900.

ArunSundar, M., Shanmugarajan, T.S., Ravichandiran, V., 2018. 3,4-Dihydroxyphenylethanol assuages cognitive impulsivity in alzheimer's disease by attuning HPA-Axis via differential crosstalk of α7 nAChR with MicroRNA-124 and HDAC6. ACS Chem. Neurosci. 9, 2904–2916. https://doi.org/10.1021/acschemneuro.7b00532.

Bac, B., Hicheri, C., Weiss, C., Buell, A., Vilcek, N., Spaeni, C., Geula, C., Savas, J.N., Disterhoft, J.F., 2023. The TgF344-AD rat: behavioral and proteomic changes associated with aging and protein expression in a transgenic rat model of Alzheimer's disease. Neurobiol. Aging 123, 98–110. https://doi.org/10.1016/j.neurobiolaging.2022.12.015.

Bachman, D.L., Wolf, P.A., Linn, R., Knoefel, J.E., Cobb, J., Belanger, A., D'Agostino, R. B., White, L.R., 1992. Prevalence of dementia and probable senile dementia of the Alzheimer type in the Framingham Study. Neurology 42, 115–119. https://doi.org/10.1212/wnl.42.1.115.

Baddeley, A.D., Logie, R., Bressi, S., Sala, S.D., Spinnler, H., 2017. Dementia and working memory. In: Exploring Working Memory. Routledge. Routledge, Abingdon, Oxon ; New York, NY, pp. 280–294. https://doi.org/10.4324/9781315111261-22, 2017. | Series: World library of psychologists.

Bailey, M.R., Simpson, E.H., Balsam, P.D., 2016. Neural substrates underlying effort, time, and risk-based decision making in motivated behavior. Neurobiol. Learn. Mem. 133, 233–256. https://doi.org/10.1016/j.nlm.2016.07.015.

Bañuelos, C., Beas, B.S., McQuail, J.A., Gilbert, R.J., Frazier, C.J., Setlow, B., Bizon, J.L., 2014. Prefrontal cortical GABAergic dysfunction contributes to age-related working memory impairment. J. Neurosci. 34, 3457–3466. https://doi.org/10.1523/JNEUROSCI.5192-13.2014.

Barr, A.M., Phillips, A.G., 1999. Withdrawal following repeated exposure to d-amphetamine decreases responding for a sucrose solution as measured by a progressive ratio schedule of reinforcement. Psychopharmacology (Berl) 141, 99–106. https://doi.org/10.1007/s002130050812.

Beagle, A.J., Zahir, A., Borzello, M., Kayser, A.S., Hsu, M., Miller, B.L., Kramer, J.H., Chiong, W., 2020. Amount and delay insensitivity during intertemporal choice in three neurodegenerative diseases reflects dorsomedial prefrontal atrophy. Cortex 124, 54–65. https://doi.org/10.1016/j.cortex.2019.10.009.

Beas, B.S., McQuail, J.A., Ban Uelos, C., Setlow, B., Bizon, J.L., 2017. Prefrontal cortical GABAergic signaling and impaired behavioral flexibility in aged F344 rats. Neuroscience 345, 274–286. https://doi.org/10.1016/j.neuroscience.2016.02.014.

Beas, B.S., Setlow, B., Bizon, J.L., 2016. Effects of acute administration of the GABA(B) receptor agonist baclofen on behavioral flexibility in rats. Psychopharmacology (Berl) 233, 2787–2797. https://doi.org/10.1007/s00213-016-4321-y.

Beas, B.S., Setlow, B., Bizon, J.L., 2013. Distinct manifestations of executive dysfunction in aged rats. Neurobiol. Aging 34, 2164–2174. https://doi.org/10.1016/j.neurobiolaging.2013.03.019.

Belfiore, R., Rodin, A., Ferreira, E., Velazquez, R., Branca, C., Caccamo, A., Oddo, S., 2019. Temporal and regional progression of Alzheimer's disease-like pathology in 3xTg-AD mice. Aging Cell 18, e12873. https://doi.org/10.1111/acel.12873.

Berkowitz, L.E., Harvey, R.E., Drake, E., Thompson, S.M., Clark, B.J., 2018. Progressive impairment of directional and spatially precise trajectories by TgF344-Alzheimer's disease rats in the Morris Water Task. Sci. Rep. 8, 16153 https://doi.org/10.1038/s41598-018-34368-w.

Bernaud, V.E., Bulen, H.L., Peña, V.L., Koebele, S.V., Northup-Smith, S.N., Manzo, A.A., Valenzuela Sanchez, M., Opachich, Z., Ruhland, A.M., Bimonte-Nelson, H.A., 2022. Task-dependent learning and memory deficits in the TgF344-AD rat model of Alzheimer's disease: three key timepoints through middle-age in females. Sci. Rep. 12, 14596 https://doi.org/10.1038/s41598-022-18415-1.

Bertoux, M., de Souza, L.C., Zamith, P., Dubois, B., Bourgeois-Gironde, S., 2015. Discounting of future rewards in behavioural variant frontotemporal dementia and Alzheimer's disease. Neuropsychology 29, 933–939. https://doi.org/10.1037/neu0000197.

Bettcher, B.M., Kramer, J.H., 2014. Longitudinal inflammation, cognitive decline, and Alzheimer's disease: a mini-review. Clin. Pharmacol. Ther. 96, 464–469. https://doi.org/10.1038/clpt.2014.147.

Blokland, A., Ten Oever, S., van Gorp, D., van Draanen, M., Schmidt, T., Nguyen, E., Krugliak, J., Napoletano, A., Keuter, S., Klinkenberg, I., 2012. The use of a test battery assessing affective behavior in rats: order effects. Behav. Brain Res. 228, 16–21. https://doi.org/10.1016/j.bbr.2011.11.042.

Bobova, L., Finn, P.R., Rickert, M.E., Lucas, J., 2009. Disinhibitory psychopathology and delay discounting in alcohol dependence: personality and cognitive correlates. Exp. Clin. Psychopharmacol 17, 51–61. https://doi.org/10.1037/a0014503.

Boulougouris, V., Dalley, J.W., Robbins, T.W., 2007. Effects of orbitofrontal, infralimbic and prelimbic cortical lesions on serial spatial reversal learning in the rat. Behav. Brain Res. 179, 219–228. https://doi.org/10.1016/j.bbr.2007.02.005.

Bruce-Keller, A.J., Umberger, G., McFall, R., Mattson, M.P., 1999. Food restriction reduces brain damage and improves behavioral outcome following excitotoxic and metabolic insults. Annals of Neurology: Official Journal of the American Neurological Association and the Child Neurology Society 45 (1), 8–15.

Cardinal, R.N., Pennicott, D.R., Sugathapala, C.L., Robbins, T.W., Everitt, B.J., 2001. Impulsive choice induced in rats by lesions of the nucleus accumbens core. Science 292, 2499–2501. https://doi.org/10.1126/science.1060818.

Cerejeira, J., Lagarto, L., Mukaetova-Ladinska, E.B., 2012. Behavioral and psychological symptoms of dementia. Front. Neurol. 3, 73. https://doi.org/10.3389/fneur.2012.00073.

Cetin, T., Freudenberg, F., Füchtemeier, M., Koch, M., 2004. Dopamine in the orbitofrontal cortex regulates operant responding under a progressive ratio of reinforcement in rats. Neurosci. Lett. 370, 114–117. https://doi.org/10.1016/j.neulet.2004.08.002.

Ceyzériat, K., Gloria, Y., Tsartsalis, S., Fossey, C., Cailly, T., Fabis, F., Millet, P., Tournier, B.B., 2021. Alterations in dopamine system and in its connectivity with serotonin in a rat model of Alzheimer's disease. Brain Commun. 3, fcab029 https://doi.org/10.1093/braincomms/fcab029.

Ceyzériat, K., Jaques, E., Gloria, Y., Badina, A., Millet, P., Koutsouvelis, N., Dipasquale, G., Frisoni, G.B., Zilli, T., Garibotto, V., Tournier, B.B., 2024. Low-dose radiation therapy impacts microglial inflammatory response without modulating amyloid load in female TgF344-AD rats. J. Alzheimers Dis. https://doi.org/10.3233/JAD-231153.

Chowdhury, T.G., Fenton, A.A., Aoki, C., 2021. Effects of adolescent experience of food restriction and exercise on spatial learning and open field exploration of female rats. Hippocampus 31, 170–188. https://doi.org/10.1002/hipo.23275.

Churchwell, J.C., Morris, A.M., Heurtelou, N.M., Kesner, R.P., 2009. Interactions between the prefrontal cortex and amygdala during delay discounting and reversal. Behav. Neurosci. 123, 1185–1196. https://doi.org/10.1037/a0017734.

Coelho, S., Guerreiro, M., Chester, C., Silva, D., Maroco, J., Paglieri, F., de Mendonça, A., 2017. Delay discounting in mild cognitive impairment. J. Clin. Exp. Neuropsychol. 39, 336–346. https://doi.org/10.1080/13803395.2016.1226269.

Cohen, R.M., Rezai-Zadeh, K., Weitz, T.M., Rentsendorj, A., Gate, D., Spivak, I., Bholat, Y., Vasilevko, V., Glabe, C.G., Breunig, J.J., Rakic, P., Davtyan, H., Agadjanyan, M.G., Kepe, V., Barrio, J.R., Bannykh, S., Szekely, C.A., Pechnick, R.N., Town, T., 2013. A transgenic Alzheimer rat with plaques, tau pathology, behavioral impairment, oligomeric aβ, and frank neuronal loss. J. Neurosci. 33, 6245–6256. https://doi.org/10.1523/JNEUROSCI.3672-12.2013.

Craig, A.H., Cummings, J.L., Fairbanks, L., Itti, L., Miller, B.L., Li, J., Mena, I., 1996. Cerebral blood flow correlates of apathy in Alzheimer disease. Arch. Neurol. 53, 1116–1120. https://doi.org/10.1001/archneur.1996.00550110056012.

Dietrich, A., Allen, J.D., 1998. Functional dissociation of the prefrontal cortex and the hippocampus in timing behavior. Behav. Neurosci. 112, 1043–1047. https://doi.org/10.1037/0735-7044.112.5.1043.

DiStefano, C., Zhu, M., Mîndrilã, D., 2009. Understanding and Using Factor Scores: Considerations for the Applied Researcher. University of Massachusetts Amherst. https://doi.org/10.7275/da8t-4g52.

Dourlen, P., Fernandez-Gomez, F.J., Dupont, C., Grenier-Boley, B., Bellenguez, C., Obriot, H., Caillierez, R., Sottejeau, Y., Chapuis, J., Bretteville, A., Abdelfettah, F., Delay, C., Malmanche, N., Soininen, H., Hiltunen, M., Galas, M.C., Amouyel, P., Sergeant, N., Buée, L., Lambert, J.C., Dermaut, B., 2017. Functional screening of

Alzheimer risk loci identifies PTK2B as an in vivo modulator and early marker of Tau pathology. Mol. Psychiatr. 22, 874–883. https://doi.org/10.1038/mp.2016.59.

El Haj, M., Boutoleau-Bretonnière, C., Allain, P., 2020. Memory of decisions: relationship between decline of autobiographical memory and temporal discounting in Alzheimer's disease. J. Clin. Exp. Neuropsychol. 42, 415–424. https://doi.org/10.1080/13803395.2020.1744527.

El Haj, M., Boutoleau-Bretonnière, C., Moustafa, A., Allain, P., 2022. The discounted future: relationship between temporal discounting and future thinking in Alzheimer's disease. Appl. Neuropsychol. Adult 29, 412–418. https://doi.org/10.1080/23279095.2020.1764958.

Elkhatib, S.K., Moshfegh, C.M., Watson, G.F., Case, A.J., 2020. Peripheral inflammation is strongly linked to elevated zero maze behavior in repeated social defeat stress. Brain Behav. Immun. 90, 279–285. https://doi.org/10.1016/j.bbi.2020.08.031.

Evenden, J.L., Ryan, C.N., 1996. The pharmacology of impulsive behaviour in rats: the effects of drugs on response choice with varying delays of reinforcement. Psychopharmacology (Berl) 128, 161–170. https://doi.org/10.1007/s002130050121.

Fabrigoule, C., Letenneur, L., Dartigues, J.F., Zarrouk, M., Commenges, D., Barberger-Gateau, P., 1995. Social and leisure activities and risk of dementia: a prospective longitudinal study. J. Am. Geriatr. Soc. 43, 485–490. https://doi.org/10.1111/j.1532-5415.1995.tb06093.x.

Fernandez, N.F., Gundersen, G.W., Rahman, A., Grimes, M.L., Rikova, K., Hornbeck, P., Ma'ayan, A., 2017. Clustergrammer, a web-based heatmap visualization and analysis tool for high-dimensional biological data. Sci. Data 4, 170151. https://doi.org/10.1038/sdata.2017.151.

Floresco, S.B., Block, A.E., Tse, M.T.L., 2008a. Inactivation of the medial prefrontal cortex of the rat impairs strategy set-shifting, but not reversal learning, using a novel, automated procedure. Behav. Brain Res. 190, 85–96. https://doi.org/10.1016/j.bbr.2008.02.008.

Floresco, S.B., Magyar, O., 2006. Mesocortical dopamine modulation of executive functions: beyond working memory. Psychopharmacology (Berl) 188, 567–585. https://doi.org/10.1007/s00213-006-0404-5.

Floresco, S.B., St Onge, J.R., Ghods-Sharifi, S., Winstanley, C.A., 2008b. Cortico-limbic-striatal circuits subserving different forms of cost-benefit decision making. Cognit. Affect Behav. Neurosci. 8, 375–389. https://doi.org/10.3758/CABN.8.4.375.

Floresco, S.B., 2013. Prefrontal dopamine and behavioral flexibility: shifting from an "inverted-U" toward a family of functions. Front. Neurosci. 7, 62. https://doi.org/10.3389/fnins.2013.00062.

Fobbs, W.C., Mizumori, S.J.Y., 2017. A framework for understanding and advancing intertemporal choice research using rodent models. Neurobiol. Learn. Mem. 139, 89–97. https://doi.org/10.1016/j.nlm.2017.01.004.

Forny-Germano, L., Lyra e Silva, N.M., Batista, A.F., Brito-Moreira, J., Gralle, M., Boehnke, S.E., Coe, B.C., Lablans, A., Marques, S.A., Martinez, A.M.B., Klein, W.L., Houzel, J.-C., Ferreira, S.T., Munoz, D.P., De Felice, F.G., 2014. Alzheimer's disease-like pathology induced by amyloid-β oligomers in nonhuman primates. J. Neurosci. 34, 13629–13643. https://doi.org/10.1523/JNEUROSCI.1353-14.2014.

Fratiglioni, L., Viitanen, M., von Strauss, E., Tontodonati, V., Herlitz, A., Winblad, B., 1997. Very old women at highest risk of dementia and Alzheimer's disease: incidence data from the Kungsholmen Project, Stockholm. Neurology 48, 132–138. https://doi.org/10.1212/wnl.48.1.132.

Galimberti, D., Fenoglio, C., Lovati, C., Venturelli, E., Guidi, I., Corrà, B., Scalabrini, D., Clerici, F., Mariani, C., Bresolin, N., Scarpini, E., 2006. Serum MCP-1 levels are increased in mild cognitive impairment and mild Alzheimer's disease. Neurobiol. Aging 27, 1763–1768. https://doi.org/10.1016/j.neurobiolaging.2005.10.007.

Gambassi, G., Lapane, K.L., Landi, F., Sgadari, A., Mor, V., Bernabei, R., 1999. Gender differences in the relation between comorbidity and mortality of patients with Alzheimer's disease. Neurology 53, 508. https://doi.org/10.1212/WNL.53.3.508, 508.

Geng, Z., Wu, X., Wang, L., Zhou, S., Tian, Y., Wang, K., Wei, L., 2020. Reduced delayed reward selection by Alzheimer's disease and mild cognitive impairment patients during intertemporal decision-making. J. Clin. Exp. Neuropsychol. 42, 298–306. https://doi.org/10.1080/13803395.2020.1711873.

Goodman, A.M., Langner, B.M., Jackson, N., Alex, C., McMahon, L.L., 2021. Heightened hippocampal β-adrenergic receptor function drives synaptic potentiation and supports learning and memory in the TgF344-AD rat model during prodromal alzheimer's disease. J. Neurosci. 41, 5747–5761. https://doi.org/10.1523/JNEUROSCI.0119-21.2021.

Grammas, P., Ovase, R., 2001. Inflammatory factors are elevated in brain microvessels in Alzheimer's disease. Neurobiol. Aging 22, 837–842. https://doi.org/10.1016/s0197-4580(01)00276-7.

Gunn, R.L., Finn, P.R., 2013. Impulsivity partially mediates the association between reduced working memory capacity and alcohol problems. Alcohol 47, 3–8. https://doi.org/10.1016/j.alcohol.2012.10.003.

Gustavsson, A., Norton, N., Fast, T., Frölich, L., Georges, J., Holzapfel, D., Kirabali, T., Krolak-Salmon, P., Rossini, P.M., Ferretti, M.T., Lanman, L., Chadha, A.S., van der Flier, W.M., 2023. Global estimates on the number of persons across the Alzheimer's disease continuum. Alzheimers Dement 19, 658–670. https://doi.org/10.1002/alz.12694.

Hamann, S., Monarch, E.S., Goldstein, F.C., 2002. Impaired fear conditioning in Alzheimer's disease. Neuropsychologia 40, 1187–1195. https://doi.org/10.1016/s0028-3932(01)00223-8.

Heiderstadt, K.M., McLaughlin, R.M., Wright, D.C., Walker, S.E., Gomez-Sanchez, C.E., 2000. The effect of chronic food and water restriction on open-field behaviour and serum corticosterone levels in rats. Lab. Anim. 34, 20–28. https://doi.org/10.1258/002367700780578028.

Hernandez, A.R., Hernandez, C.M., Campos, K., Truckenbrod, L., Federico, Q., Moon, B., McQuail, J.A., Maurer, A.P., Bizon, J.L., Burke, S.N., 2018a. A ketogenic diet improves cognition and has biochemical effects in prefrontal cortex that are dissociable from hippocampus. Front. Aging Neurosci. 10, 391. https://doi.org/10.3389/fnagi.2018.00391.

Hernandez, A.R., Hernandez, C.M., Campos, K.T., Truckenbrod, L.M., Sakarya, Y., McQuail, J.A., Carter, C.S., Bizon, J.L., Maurer, A.P., Burke, S.N., 2018b. The antiepileptic ketogenic diet alters hippocampal transporter levels and reduces adiposity in aged rats. J. Gerontol. A Biol. Sci. Med. Sci. 73, 450–458. https://doi.org/10.1093/gerona/glx193.

Hernandez, C.M., Jackson, N.L., Hernandez, A.R., McMahon, L.L., 2022a. Impairments in fear extinction memory and basolateral amygdala plasticity in the TgF344-AD rat model of alzheimer's disease are distinct from nonpathological aging. eNeuro 9. https://doi.org/10.1523/ENEURO.0181-22.2022.

Hernandez, C.M., McQuail, J.A., Schwabe, M.R., Burke, S.N., Setlow, B., Bizon, J.L., 2018. Age-related declines in prefrontal cortical expression of metabotropic glutamate receptors that support working memory. eNeuro 5. https://doi.org/10.1523/ENEURO.0164-18.2018.

Hernandez, C.M., McQuail, J.A., Ten Eyck, T.W., Wheeler, A.-R., Labiste, C.C., Setlow, B., Bizon, J.L., 2022b. GABAB receptors in prelimbic cortex and basolateral amygdala differentially influence intertemporal decision making and decline with age. Neuropharmacology 209, 109001. https://doi.org/10.1016/j.neuropharm.2022.109001.

Hernandez, C.M., Orsini, C.A., Labiste, C.C., Wheeler, A.-R., Ten Eyck, T.W., Bruner, M.M., Sahagian, T.J., Harden, S.W., Frazier, C.J., Setlow, B., Bizon, J.L., 2019. Optogenetic dissection of basolateral amygdala contributions to intertemporal choice in young and aged rats. Elife 8. https://doi.org/10.7554/eLife.46174.

Hernandez, C.M., Vetere, L.M., Orsini, C.A., McQuail, J.A., Maurer, A.P., Burke, S.N., Setlow, B., Bizon, J.L., 2017. Decline of prefrontal cortical-mediated executive functions but attenuated delay discounting in aged Fischer 344 × brown Norway hybrid rats. Neurobiol. Aging 60, 141–152. https://doi.org/10.1016/j.neurobiolaging.2017.08.025.

Herzig, M.C., Winkler, D.T., Burgermeister, P., Pfeifer, M., Kohler, E., Schmidt, S.D., Danner, S., Abramowski, D., Stürchler-Pierrat, C., Bürki, K., van Duinen, S.G., Maat-Schieman, M.L.C., Staufenbiel, M., Mathews, P.M., Jucker, M., 2004. Abeta is targeted to the vasculature in a mouse model of hereditary cerebral hemorrhage with amyloidosis. Nat. Neurosci. 7, 954–960. https://doi.org/10.1038/nn1302.

Hoefer, M., Allison, S.C., Schauer, G.F., Neuhaus, J.M., Hall, J., Dang, J.N., Weiner, M.W., Miller, B.L., Rosen, H.J., 2008. Fear conditioning in frontotemporal lobar degeneration and Alzheimer's disease. Brain 131, 1646–1657. https://doi.org/10.1093/brain/awn082.

Holmes, C., Cunningham, C., Zotova, E., Woolford, J., Dean, C., Kerr, S., Culliford, D., Perry, V.H., 2009. Systemic inflammation and disease progression in Alzheimer disease. Neurology 73, 768–774. https://doi.org/10.1212/WNL.0b013e3181b6bb95.

Huckans, M., Seelye, A., Woodhouse, J., Parcel, T., Mull, L., Schwartz, D., Mitchell, A., Lahna, D., Johnson, A., Loftis, J., Woods, S.P., Mitchell, S.H., Hoffman, W., 2011. Discounting of delayed rewards and executive dysfunction in individuals infected with hepatitis C. J. Clin. Exp. Neuropsychol. 33, 176–186. https://doi.org/10.1080/13803395.2010.499355.

Hui-Yin, Y., 2014. Insignificant influence of test order on cognitive behavior in Wistar rats. J. Pharm. Negat. Results 5, 29–33.

Inagaki, T.K., Muscatell, K.A., Irwin, M.R., Cole, S.W., Eisenberger, N.I., 2012. Inflammation selectively enhances amygdala activity to socially threatening images. Neuroimage 59, 3222–3226. https://doi.org/10.1016/j.neuroimage.2011.10.090.

Jansen, W.J., Wilson, R.S., Visser, P.J., Nag, S., Schneider, J.A., James, B.D., Leurgans, S.E., Capuano, A.W., Bennett, D.A., Boyle, P.A., 2018. Age and the association of dementia-related pathology with trajectories of cognitive decline. Neurobiol. Aging 61, 138–145. https://doi.org/10.1016/j.neurobiolaging.2017.08.029.

Kelberman, M.A., Anderson, C.R., Chlan, E., Rorabaugh, J.M., McCann, K.E., Weinshenker, D., 2022. Consequences of hyperphosphorylated tau in the locus coeruleus on behavior and cognition in a rat model of alzheimer's disease. J. Alzheimers Dis. 86, 1037–1059. https://doi.org/10.3233/JAD-215546.

Kenny, R., Dinan, T., Cai, G., Spencer, S.J., 2014. Effects of mild calorie restriction on anxiety and hypothalamic-pituitary-adrenal axis responses to stress in the male rat. Phys. Rep. 2, e00265 https://doi.org/10.1002/phy2.265.

Kheramin, S., Body, S., Herrera, F.M., Bradshaw, C.M., Szabadi, E., Deakin, J.F.W., Anderson, I.M., 2005. The effect of orbital prefrontal cortex lesions on performance on a progressive ratio schedule: implications for models of inter-temporal choice. Behav. Brain Res. 156, 145–152. https://doi.org/10.1016/j.bbr.2004.05.017.

Koenig, A.M., Arnold, S.E., Streim, J.E., 2016. Agitation and irritability in alzheimer's disease: evidenced-based treatments and the black-box warning. Curr. Psychiatr. Rep. 18, 3. https://doi.org/10.1007/s11920-015-0640-7.

Kumar, R., Nordberg, A., Darreh-Shori, T., 2016. Amyloid-β peptides act as allosteric modulators of cholinergic signalling through formation of soluble BAβACs. Brain 139, 174–192. https://doi.org/10.1093/brain/awv318.

Kuzis, G., Sabe, L., Tiberti, C., Dorrego, F., Starkstein, S.E., 1999. Neuropsychological correlates of apathy and depression in patients with dementia. Neurology 52, 1403–1407. https://doi.org/10.1212/wnl.52.7.1403.

Lafleche, G., Albert, M.S., 1995. Executive function deficits in mild Alzheimer's disease. Neuropsychology 9, 313–320. https://doi.org/10.1037/0894-4105.9.3.313.

Lai, K.S.P., Liu, C.S., Rau, A., Lanctôt, K.L., Köhler, C.A., Pakosh, M., Carvalho, A.F., Herrmann, N., 2017. Peripheral inflammatory markers in Alzheimer's disease: a systematic review and meta-analysis of 175 studies. J. Neurol. Neurosurg. Psychiatr. 88, 876–882. https://doi.org/10.1136/jnnp-2017-316201.

Lanzrein, A.S., Johnston, C.M., Perry, V.H., Jobst, K.A., King, E.M., Smith, A.D., 1998. Longitudinal study of inflammatory factors in serum, cerebrospinal fluid, and brain tissue in Alzheimer disease: interleukin-1beta, interleukin-6, interleukin-1 receptor antagonist, tumor necrosis factor-alpha, the soluble tumor necrosis factor receptors I and II, and alpha1-antichymotrypsin. Alzheimer Dis. Assoc. Disord. 12, 215–227. https://doi.org/10.1097/00002093-199809000-00016.

Leung, R., Proitsi, P., Simmons, A., Lunnon, K., Güntert, A., Kronenberg, D., Pritchard, M., Tsolaki, M., Mecocci, P., Kloszewska, I., Vellas, B., Soininen, H., Wahlund, L.-O., Lovestone, S., 2013. Inflammatory proteins in plasma are associated with severity of Alzheimer's disease. PLoS One 8, e64971. https://doi.org/10.1371/journal.pone.0064971.

Levin, F., Jelistratova, I., Betthauser, T.J., Okonkwo, O., Johnson, S.C., Teipel, S.J., Grothe, M.J., 2021. In vivo staging of regional amyloid progression in healthy middle-aged to older people at risk of Alzheimer's disease. Alzheimer's Res. Ther. 13, 178. https://doi.org/10.1186/s13195-021-00918-0.

Levy, M.L., Cummings, J.L., Fairbanks, L.A., Masterman, D., Miller, B.L., Craig, A.H., Paulsen, J.S., Litvan, I., 1998. Apathy is not depression. J. Neuropsychiatry Clin. Neurosci. 10, 314–319. https://doi.org/10.1176/jnp.10.3.314.

Liu, B., Su, M., Tang, S., Zhou, X., Zhan, H., Yang, F., Li, W., Li, T., Xie, J., 2016. Spinal astrocytic activation contributes to mechanical allodynia in a rat model of cyclophosphamide-induced cystitis. Mol. Pain 12. https://doi.org/10.1177/1744806916674479.

Liu, X., Zhou, Q., Zhang, J.-H., Wang, K.-Y., Saito, T., Saido, T.C., Wang, X., Gao, X., Azuma, K., 2021. Microglia-based sex-biased neuropathology in early-stage alzheimer's disease model mice and the potential pharmacologic efficacy of dioscin. Cells 10. https://doi.org/10.3390/cells10113261.

Lue, L.F., Rydel, R., Brigham, E.F., Yang, L.B., Hampel, H., Murphy, G.M., Brachova, L., Yan, S.D., Walker, D.G., Shen, Y., Rogers, J., 2001. Inflammatory repertoire of Alzheimer's disease and nondemented elderly microglia in vitro. Glia 35, 72–79. https://doi.org/10.1002/glia.1072.

Maddox, W.T., Markman, A.B., 2010. The motivation-cognition interface in learning and decision-making. Curr. Dir. Psychol. Sci. 19, 106–110. https://doi.org/10.1177/0963721410364008.

Maes, M., DeVos, N., Wauters, A., Demedts, P., Maurits, V., Neels, H., Bosmans, E., Altamura, C., Lin, A., Song, C., Vandenbroucke, M., Scharpe, S., 1999. Inflammatory markers in younger vs elderly normal volunteers and in patients with Alzheimer's disease. J. Psychiatr. Res. 33, 397–405. https://doi.org/10.1016/S0022-3956(99)00016-3.

Malá, H., Andersen, L.G., Christensen, R.F., Felbinger, A., Hagstrøm, J., Meder, D., Pearce, H., Mogensen, J., 2015. Prefrontal cortex and hippocampus in behavioural flexibility and posttraumatic functional recovery: reversal learning and set-shifting in rats. Brain Res. Bull. 116, 34–44. https://doi.org/10.1016/j.brainresbull.2015.05.006.

Mann, R.S., 1990. Differential diagnosis and classification of apathy. Am. J. Psychiatr. 147, 22–30.

Manuel, A.L., Roquet, D., Landin-Romero, R., Kumfor, F., Ahmed, R.M., Hodges, J.R., Piguet, O., 2020. Interactions between decision-making and emotion in behavioral-variant frontotemporal dementia and Alzheimer's disease. Soc. Cognit. Affect Neurosci. 15, 681–694. https://doi.org/10.1093/scan/nsaa085.

Masuda, A., Kobayashi, Y., Kogo, N., Saito, T., Saido, T.C., Itohara, S., 2016. Cognitive deficits in single App knock-in mouse models. Neurobiol. Learn. Mem. 135, 73–82. https://doi.org/10.1016/j.nlm.2016.07.001.

McPherson, S., Fairbanks, L., Tiken, S., Cummings, J.L., Back-Madruga, C., 2002. Apathy and executive function in Alzheimer's disease. J. Int. Neuropsychol. Soc. 8, 373–381. https://doi.org/10.1017/s1355617702813182.

McQuail, J.A., Beas, B.S., Kelly, K.B., Simpson, K.L., Frazier, C.J., Setlow, B., Bizon, J.L., 2016. NR2A-Containing NMDARs in the prefrontal cortex are required for working memory and associated with age-related cognitive decline. J. Neurosci. 36, 12537–12548. https://doi.org/10.1523/JNEUROSCI.2332-16.2016.

Mendez, I.A., Williams, M.T., Bhavsar, A., Lu, A.P., Bizon, J.L., Setlow, B., 2009. Long-lasting sensitization of reward-directed behavior by amphetamine. Behav. Brain Res. 201, 74–79. https://doi.org/10.1016/j.bbr.2009.01.034.

Mendez, M.F., Martin, R.J., Smyth, K.A., Whitehouse, P.J., 1992. Disturbances of person identification in Alzheimer's disease. A retrospective study. J. Nerv. Ment. Dis. 180, 94–96. https://doi.org/10.1097/00005053-199202000-00005.

Miyamoto, T., Kim, D., Knox, J.A., Johnson, E., Mucke, L., 2016. Increasing the receptor tyrosine kinase EphB2 prevents amyloid-β-induced depletion of cell surface glutamate receptors by a mechanism that requires the PDZ-binding motif of EphB2 and neuronal activity. J. Biol. Chem. 291, 1719–1734. https://doi.org/10.1074/jbc.M115.666529.

Mondadori, C.R.A., Buchmann, A., Mustovic, H., Schmidt, C.F., Boesiger, P., Nitsch, R.M., Hock, C., Streffer, J., Henke, K., 2006. Enhanced brain activity may precede the diagnosis of Alzheimer's disease by 30 years. Brain 129, 2908–2922. https://doi.org/10.1093/brain/awl266.

Morris, R.G., 1994. Working memory in Alzheimer-type dementia. Neuropsychology 8, 544–554. https://doi.org/10.1037/0894-4105.8.4.544.

Muñoz-Moreno, E., Tudela, R., López-Gil, X., Soria, G., 2018. Early brain connectivity alterations and cognitive impairment in a rat model of Alzheimer's disease. Alzheimer's Res. Ther. 10, 16. https://doi.org/10.1186/s13195-018-0346-2.

Nagarajan, A., Srivastava, H., Morrow, C.D., Sun, L.Y., 2023. Characterizing the gut microbiome changes with aging in a novel Alzheimer's disease rat model. Aging (Albany NY) 15, 459–471. https://doi.org/10.18632/aging.204484.

Nelson, M.E., Jester, D.J., Petkus, A.J., Andel, R., 2021. Cognitive reserve, alzheimer's neuropathology, and risk of dementia: a systematic review and meta-analysis. Neuropsychol. Rev. 31, 233–250. https://doi.org/10.1007/s11065-021-09478-4.

Nies, S.H., Takahashi, H., Herber, C.S., Huttner, A., Chase, A., Strittmatter, S.M., 2021. Spreading of Alzheimer tau seeds is enhanced by aging and template matching with limited impact of amyloid-β. J. Biol. Chem. 297, 101159 https://doi.org/10.1016/j.jbc.2021.101159.

O'Bryant, S.E., Lista, S., Rissman, R.A., Edwards, M., Zhang, F., Hall, J., Zetterberg, H., Lovestone, S., Gupta, V., Graff-Radford, N., Martins, R., Jeromin, A., Waring, S., Oh, E., Kling, M., Baker, L.D., Hampel, H., 2016. Comparing biological markers of Alzheimer's disease across blood fraction and platforms: comparing apples to oranges. Alzheimers Dement (Amst) 3, 27–34. https://doi.org/10.1016/j.dadm.2015.12.003.

Oddo, S., Caccamo, A., Green, K.N., Liang, K., Tran, L., Chen, Y., Leslie, F.M., LaFerla, F.M., 2005. Chronic nicotine administration exacerbates tau pathology in a transgenic model of Alzheimer's disease. Proc. Natl. Acad. Sci. U.S.A. 102, 3046–3051. https://doi.org/10.1073/pnas.0408500102.

Orsini, C., Buchini, F., Conversi, D., Cabib, S., 2004. Selective improvement of strain-dependent performances of cognitive tasks by food restriction. Neurobiol. Learn. Mem. 81, 96–99. https://doi.org/10.1016/s1074-7427(03)00075-3.

Orsini, C.A., Moorman, D.E., Young, J.W., Setlow, B., Floresco, S.B., 2015. Neural mechanisms regulating different forms of risk-related decision-making: insights from animal models. Neurosci. Biobehav. Rev. 58, 147–167. https://doi.org/10.1016/j.neubiorev.2015.04.009.

Parikh, I., Guo, J., Chuang, K.-H., Zhong, Y., Rempe, R.G., Hoffman, J.D., Armstrong, R., Bauer, B., Hartz, A.M.S., Lin, A.-L., 2016. Caloric restriction preserves memory and reduces anxiety of aging mice with early enhancement of neurovascular functions. Aging (Albany NY) 8, 2814–2826. https://doi.org/10.18632/aging.101094.

Pascoal, T.A., Benedet, A.L., Ashton, N.J., Kang, M.S., Therriault, J., Chamoun, M., Savard, M., Lussier, F.Z., Tissot, C., Karikari, T.K., Ottoy, J., Mathotaarachchi, S., Stevenson, J., Massarweh, G., Schöll, M., de Leon, M.J., Soucy, J.-P., Edison, P., Blennow, K., Zetterberg, H., Gauthier, S., Rosa-Neto, P., 2021. Microglial activation and tau propagate jointly across Braak stages. Nat. Med. 27, 1592–1599. https://doi.org/10.1038/s41591-021-01456-w.

Patel, D.C., Wallis, G., Dahle, E.J., McElroy, P.B., Thomson, K.E., Tesi, R.J., Szymkowski, D.E., West, P.J., Smeal, R.M., Patel, M., Fujinami, R.S., White, H.S., Wilcox, K.S., 2017. Hippocampal TNFα signaling contributes to seizure generation in an infection-induced mouse model of limbic epilepsy. eNeuro 4. https://doi.org/10.1523/ENEURO.0105-17.2017.

Patel, N.S., Paris, D., Mathura, V., Quadros, A.N., Crawford, F.C., Mullan, M.J., 2005. Inflammatory cytokine levels correlate with amyloid load in transgenic mouse models of Alzheimer's disease. J. Neuroinflammation 2, 9. https://doi.org/10.1186/1742-2094-2-9.

Peters, J., Büchel, C., 2011. The neural mechanisms of inter-temporal decision-making: understanding variability. Trends Cognit. Sci. 15, 227–239. https://doi.org/10.1016/j.tics.2011.03.002.

Popp, J., Oikonomidi, A., Tautvydaitė, D., Dayon, L., Bacher, M., Migliavacca, E., Henry, H., Kirkland, R., Severin, I., Wojcik, J., Bowman, G.L., 2017. Markers of neuroinflammation associated with Alzheimer's disease pathology in older adults. Brain Behav. Immun. 62, 203–211. https://doi.org/10.1016/j.bbi.2017.01.020.

Reed, B.R., Mungas, D., Farias, S.T., Harvey, D., Beckett, L., Widaman, K., Hinton, L., DeCarli, C., 2010. Measuring cognitive reserve based on the decomposition of episodic memory variance. Brain 133, 2196–2209. https://doi.org/10.1093/brain/awq154.

Resnick, B., Zimmerman, S.I., Magaziner, J., Adelman, A., 1998. Use of the Apathy Evaluation Scale as a measure of motivation in elderly people. Rehabil. Nurs. 23, 141–147. https://doi.org/10.1002/j.2048-7940.1998.tb01766.x.

Riul, T.R., Almeida, S.S., 2020. Feed restriction since lactation has reduced anxiety in adult Wistar rats. Rev. Nutr. 33 https://doi.org/10.1590/1678-9865202033e190143.

Robert, P., Onyike, C.U., Leentjens, A.F.G., Dujardin, K., Aalten, P., Starkstein, S., Verhey, F.R.J., Yessavage, J., Clement, J.P., Drapier, D., Bayle, F., Benoit, M., Boyer, P., Lorca, P.M., Thibaut, F., Gauthier, S., Grossberg, G., Vellas, B., Byrne, J., 2009. Proposed diagnostic criteria for apathy in Alzheimer's disease and other neuropsychiatric disorders. Eur. Psychiatr. 24, 98–104. https://doi.org/10.1016/j.eurpsy.2008.09.001.

Rorabaugh, J.M., Chalermpalanupap, T., Botz-Zapp, C.A., Fu, V.M., Lembeck, N.A., Cohen, R.M., Weinshenker, D., 2017. Chemogenetic locus coeruleus activation restores reversal learning in a rat model of Alzheimer's disease. Brain 140, 3023–3038. https://doi.org/10.1093/brain/awx232.

Sabaie, H., Tamimi, P., Gharesouran, J., Salkhordeh, Z., Asadi, M.R., Sharifi-Bonab, M., Shirvani-Farsani, Z., Taheri, M., Sayad, A., Rezazadeh, M., 2023. Expression analysis of inhibitory B7 family members in Alzheimer's disease. Metab. Brain Dis. 38, 2563–2572. https://doi.org/10.1007/s11011-023-01274-8.

Scarmeas, N., Stern, Y., 2003. Cognitive reserve and lifestyle. J. Clin. Exp. Neuropsychol. 25, 625–633. https://doi.org/10.1076/jcen.25.5.625.14576.

Shamosh, N.A., Deyoung, C.G., Green, A.E., Reis, D.L., Johnson, M.R., Conway, A.R.A., Engle, R.W., Braver, T.S., Gray, J.R., 2008. Individual differences in delay discounting: relation to intelligence, working memory, and anterior prefrontal cortex. Psychol. Sci. 19, 904–911. https://doi.org/10.1111/j.1467-9280.2008.02175.x.

Shimp, K.G., Mitchell, M.R., Beas, B.S., Bizon, J.L., Setlow, B., 2015. Affective and cognitive mechanisms of risky decision making. Neurobiol. Learn. Mem. 117, 60–70. https://doi.org/10.1016/j.nlm.2014.03.002.

Shokouhi, S., Conley, A.C., Baker, S.L., Albert, K., Kang, H., Gwirtsman, H.E., Newhouse, P.A., Alzheimer's Disease Neuroimaging Initiative, 2019. The relationship between domain-specific subjective cognitive decline and Alzheimer's pathology in normal elderly adults. Neurobiol. Aging 81, 22–29. https://doi.org/10.1016/j.neurobiolaging.2019.05.011.

Simon, N.W., LaSarge, C.L., Montgomery, K.S., Williams, M.T., Mendez, I.A., Setlow, B., Bizon, J.L., 2010. Good things come to those who wait: attenuated discounting of delayed rewards in aged Fischer 344 rats. Neurobiol. Aging 31, 853–862. https://doi.org/10.1016/j.neurobiolaging.2008.06.004.

Sloan, H.L., Good, M., Dunnett, S.B., 2006. Double dissociation between hippocampal and prefrontal lesions on an operant delayed matching task and a water maze reference memory task. Behav. Brain Res. 171, 116–126. https://doi.org/10.1016/j.bbr.2006.03.030.

Smith, L.A., Goodman, A.M., McMahon, L.L., 2022. Dentate granule cells are hyperexcitable in the TgF344-AD rat model of alzheimer's disease. Front. Synaptic Neurosci. 14, 826601 https://doi.org/10.3389/fnsyn.2022.826601.

Smith, L.A., McMahon, L.L., 2018. Deficits in synaptic function occur at medial perforant path-dentate granule cell synapses prior to Schaffer collateral-CA1 pyramidal cell synapses in the novel TgF344-Alzheimer's Disease Rat Model. Neurobiol. Dis. 110, 166–179. https://doi.org/10.1016/j.nbd.2017.11.014.

Srivastava, H., Lasher, A.T., Nagarajan, A., Sun, L.Y., 2023. Sexual dimorphism in the peripheral metabolic homeostasis and behavior in the TgF344-AD rat model of Alzheimer's disease. Aging Cell 22, e13854. https://doi.org/10.1111/acel.13854.

Stargardt, A., Swaab, D.F., Bossers, K., 2015. Storm before the quiet: neuronal hyperactivity and Aβ in the presymptomatic stages of Alzheimer's disease. Neurobiol. Aging 36, 1–11. https://doi.org/10.1016/j.neurobiolaging.2014.08.014.

Stewart, J., Mitchell, J., Kalant, N., 1989. The effects of life-long food restriction on spatial memory in young and aged Fischer 344 rats measured in the eight-arm radial and the Morris water mazes. Neurobiol. Aging 10, 669–675. https://doi.org/10.1016/0197-4580(89)90003-1.

Stopford, C.L., Thompson, J.C., Neary, D., Richardson, A.M.T., Snowden, J.S., 2012. Working memory, attention, and executive function in Alzheimer's disease and frontotemporal dementia. Cortex 48, 429–446. https://doi.org/10.1016/j.cortex.2010.12.002.

Sutoko, S., Masuda, A., Kandori, A., Sasaguri, H., Saito, T., Saido, T.C., Funane, T., 2021. Early identification of alzheimer's disease in mouse models: application of deep neural network algorithm to cognitive behavioral parameters. iScience 24, 102198. https://doi.org/10.1016/j.isci.2021.102198.

Targa Dias Anastacio, H., Matosin, N., Ooi, L., 2022. Neuronal hyperexcitability in Alzheimer's disease: what are the drivers behind this aberrant phenotype? Transl. Psychiatry 12, 257. https://doi.org/10.1038/s41398-022-02024-7.

Tarkowski, E., Blennow, K., Wallin, A., Tarkowski, A., 1999. Intracerebral production of tumor necrosis factor-alpha, a local neuroprotective agent, in Alzheimer disease and vascular dementia. J. Clin. Immunol. 19, 223–230. https://doi.org/10.1023/a:1020568013953.

Thakker, D.R., Weatherspoon, M.R., Harrison, J., Keene, T.E., Lane, D.S., Kaemmerer, W.F., Stewart, G.R., Shafer, L.L., 2009. Intracerebroventricular amyloid-beta antibodies reduce cerebral amyloid angiopathy and associated micro-hemorrhages in aged Tg2576 mice. Proc. Natl. Acad. Sci. U.S.A. 106, 4501–4506. https://doi.org/10.1073/pnas.0813404106.

Thoma, M.V., Maercker, A., Forstmeier, S., 2017. Evidence for different trajectories of delay discounting in older adults with mild cognitive impairment and mild alzheimer's disease. J. Gerontol. B Psychol. Sci. Soc. Sci. 72, 956–965. https://doi.org/10.1093/geronb/gbw010.

Tournier, B.B., Barca, C., Fall, A.B., Gloria, Y., Meyer, L., Ceyzériat, K., Millet, P., 2021. Spatial reference learning deficits in absence of dysfunctional working memory in the TgF344-AD rat model of Alzheimer's disease. Gene Brain Behav. 20, e12712 https://doi.org/10.1111/gbb.12712.

Tsuboi, Y., Kakimoto, K., Nakajima, M., Akatsu, H., Yamamoto, T., Ogawa, K., Ohnishi, T., Daikuhara, Y., Yamada, T., 2003. Increased hepatocyte growth factor level in cerebrospinal fluid in Alzheimer's disease. Acta Neurol. Scand. 107, 81–86. https://doi.org/10.1034/j.1600-0404.2003.02089.x.

Tucker, A.M., Stern, Y., 2011. Cognitive reserve in aging. Curr. Alzheimer Res. 8, 354–360. https://doi.org/10.2174/156720511795745320.

Vemuri, P., Lesnick, T.G., Przybelski, S.A., Knopman, D.S., Preboske, G.M., Kantarci, K., Raman, M.R., Machulda, M.M., Mielke, M.M., Lowe, V.J., Senjem, M.L., Gunter, J.L., Rocca, W.A., Roberts, R.O., Petersen, R.C., Jack, C.R., 2015. Vascular and amyloid pathologies are independent predictors of cognitive decline in normal elderly. Brain 138, 761–771. https://doi.org/10.1093/brain/awu393.

Verghese, J., Lipton, R.B., Katz, M.J., Hall, C.B., Derby, C.A., Kuslansky, G., Ambrose, A.F., Sliwinski, M., Buschke, H., 2003. Leisure activities and the risk of dementia in the elderly. N. Engl. J. Med. 348, 2508–2516. https://doi.org/10.1056/NEJMoa022252.

Weintraub, S., Carrillo, M.C., Farias, S.T., Goldberg, T.E., Hendrix, J.A., Jaeger, J., Knopman, D.S., Langbaum, J.B., Park, D.C., Ropacki, M.T., Sikkes, S.A.M., Welsh-Bohmer, K.A., Bain, L.J., Brashear, R., Budur, K., Graf, A., Martenyi, F., Storck, M.S., Randolph, C., 2018. Measuring cognition and function in the preclinical stage of Alzheimer's disease. Alzheimers Dement (N Y) 4, 64–75. https://doi.org/10.1016/j.trci.2018.01.003.

Weiss, E.M., Kohler, C.G., Vonbank, J., Stadelmann, E., Kemmler, G., Hinterhuber, H., Marksteiner, J., 2008. Impairment in emotion recognition abilities in patients with mild cognitive impairment, early and moderate Alzheimer disease compared with healthy comparison subjects. Am. J. Geriatr. Psychiatr. 16, 974–980. https://doi.org/10.1097/JGP.0b013e318186bd53.

Whalley, L.J., Deary, I.J., Appleton, C.L., Starr, J.M., 2004. Cognitive reserve and the neurobiology of cognitive aging. Ageing Res. Rev. 3, 369–382. https://doi.org/10.1016/j.arr.2004.05.001.

Wilson, R.S., Bennett, D.A., Bienias, J.L., Aggarwal, N.T., Mendes De Leon, C.F., Morris, M.C., Schneider, J.A., Evans, D.A., 2002. Cognitive activity and incident AD in a population-based sample of older persons. Neurology 59, 1910–1914. https://doi.org/10.1212/01.wnl.0000036905.59156.a1.

Wimo, A., Ali, G.-C., Guerchet, M., Prince, M., Prina, M., Wu, Y.-T., International, A.D., 2015. World Alzheimer Report 2015: the global impact of dementia: an analysis of prevalence, incidence, cost and trends. Alzheimer's Dis. Int.

Wolinski, P., Ksiazek-Winiarek, D., Glabinski, A., 2022. Cytokines and neurodegeneration in epileptogenesis. Brain Sci. 12 https://doi.org/10.3390/brainsci12030380.

Wright, A.L., Zinn, R., Hohensinn, B., Konen, L.M., Beynon, S.B., Tan, R.P., Clark, I.A., Abdipranoto, A., Vissel, B., 2013. Neuroinflammation and neuronal loss precede Aβ plaque deposition in the hAPP-J20 mouse model of Alzheimer's disease. PLoS One 8, e59586. https://doi.org/10.1371/journal.pone.0059586.

Wu, C., Yang, L., Li, Y., Dong, Y., Yang, B., Tucker, L.D., Zong, X., Zhang, Q., 2020. Effects of exercise training on anxious-depressive-like behavior in alzheimer rat. Med. Sci. Sports Exerc. 52, 1456–1469. https://doi.org/10.1249/MSS.0000000000002294.

Xu, H., Yang, R., Qi, X., Dintica, C., Song, R., Bennett, D.A., Xu, W., 2019. Association of lifespan cognitive reserve indicator with dementia risk in the presence of brain pathologies. JAMA Neurol. 76, 1184–1191. https://doi.org/10.1001/jamaneurol.2019.2455.

Yang, S.-T., Shi, Y., Wang, Q., Peng, J.-Y., Li, B.-M., 2014. Neuronal representation of working memory in the medial prefrontal cortex of rats. Mol. Brain 7, 61. https://doi.org/10.1186/s13041-014-0061-2.

Yan, S.D., Chen, X., Fu, J., Chen, M., Zhu, H., Roher, A., Slattery, T., Zhao, L., Nagashima, M., Morser, J., Migheli, A., Nawroth, P., Stern, D., Schmidt, A.M., 1996. RAGE and amyloid-beta peptide neurotoxicity in Alzheimer's disease. Nature 382, 685–691. https://doi.org/10.1038/382685a0.

Yao, F., Zhang, K., Zhang, Y., Guo, Y., Li, A., Xiao, S., Liu, Q., Shen, L., Ni, J., 2018. Identification of blood biomarkers for alzheimer's disease through computational prediction and experimental validation. Front. Neurol. 9, 1158. https://doi.org/10.3389/fneur.2018.01158.

Zahodne, L.B., Manly, J.J., Brickman, A.M., Siedlecki, K.L., Decarli, C., Stern, Y., 2013. Quantifying cognitive reserve in older adults by decomposing episodic memory variance: replication and extension. J. Int. Neuropsychol. Soc. 19, 854–862. https://doi.org/10.1017/S1355617713000738.

Zaitsev, A.V., Amakhin, D.V., Dyomina, A.V., Zakharova, M.V., Ergina, J.L., Postnikova, T.Y., Diespirov, G.P., Magazanik, L.G., 2021. Synaptic dysfunction in epilepsy. J. Evol. Biochem. Physiol. 57, 542–563. https://doi.org/10.1134/S002209302103008X.